ELSEVIER

Contents lists available at ScienceDirect

# Weather and Climate Extremes

journal homepage: www.elsevier.com/locate/wace



# Attributing a deadly landslide disaster in Southeastern Brazil to human-induced climate change

Maria Lucia Ferreira Barbosa <sup>a,b</sup>, Rafaela Quintella Veiga <sup>c,d</sup>, Renata Pacheco Quevedo <sup>e</sup>, Débora Joana Dutra <sup>a</sup>, Ana Carolina Moreira Pessôa <sup>a,f</sup>, Thaís Pereira de Medeiros <sup>a</sup>, Chantelle Burton <sup>g</sup>, Yuexiao Liu <sup>h,i</sup>, Nubia Beray Armond <sup>c,d</sup>, Rafael C. de Abreu <sup>h,i</sup>, Sihan Li <sup>j</sup>, Fraser C. Lott <sup>g</sup>, Cassiano Antonio Bortolozo <sup>k</sup>, Sarah Sparrow <sup>h,i,\*</sup>, <sup>o</sup>, Liana Oighenstein Anderson <sup>a,l</sup>

- <sup>a</sup> Earth Observation and Geoinformatics Division, National Institute for Space Research-INPE, Tropical Ecosystems and Environmental Sciences Laboratory (TREES), São José dos Campos, SP, 12227-010, Brazil
- <sup>b</sup> UK Centre for Ecology & Hydrology, Wallingford, OX10 8BB, UK
- <sup>c</sup> Department of Geography, Indiana University (IU), Blooomington, Indiana, United States
- <sup>d</sup> Department of Geography, Federal University of Rio de Janeiro (UFRJ), Rio de Janeiro, Brazil
- <sup>e</sup> ENGAGE Research Group, Department of Geography and Regional Research, University of Vienna, Vienna, 1010, Austria
- f Instituto de Pesauisa Ambiental da Amazônia IPAM, Brasília, 70863-520, Brazil
- g Met Office Hadley Centre, Met Office, UK
- h Engineering Science, University of Oxford, Oxford, UK
- <sup>1</sup> Mini TESA, Holywell House, Osney Mead, OX2 0ES, Oxford e-Research Centre, UK
- J University of Sheffield, UK
- <sup>k</sup> Universidade de São Paulo (USP), Instituto de Astronomia, Geofísica e Ciências Atmosféricas (IAG), Departamento de Geofísica, Rua do Matão, 1226, Butantã, 05508-090, São Paulo, Brazil
- 1 Divisão de Observação da Terra e Geoinformática (DIOTG), Coordenação Geral de Ciências da Terra (CGCT), Instituto Nacional de Pesquisas Espaciais (INPE), Brazil

#### ARTICLE INFO

Keywords:
Extreme weather
Heavy rainfall
Natural hazard
Attribution
Land use and land cover change

#### ABSTRACT

Petrópolis was hit by a devastating disaster in February 2022, when it rained 252.8 mm within 3 h, leading to 200 lost lives and hundreds of people being displaced. Here, we aimed to attribute the extreme rainfall event that led to several landslides in Petrópolis, assess how Land Use and Land Cover changes (LUCC) from 1985 to 2021 contributed to it, and quantify their socioeconomic impacts. For this, we compared natural-only forcing (NAT) and natural and anthropogenic forcing combined (ALL) scenarios of the HadGEM3 ensemble models with observation data. We computed the trends in LUCC and quantified the landslide's socioeconomic impacts from official datasets. Human-induced climate change made this extreme event 45 % and 71 % more likely in short and long-term rainfall, respectively. Recurrence period dropped from 2.36 years (NAT) to 1.63 years (ALL) in the short-term and from 5.66 years (NAT) to 3.31 years (ALL) in the long-term. Landscape trends show an increase in forest formations, but unprotected hilltops that collapsed presented more than 40 % of their area as farming. The total economic loss was more than USD 22 million, with 1 078 people directly affected. The study's findings are valuable in understanding how changes in extreme weather events and land use are affecting our society. We highlight the need for adaptation measures and for more research addressing the attribution of extreme events, especially those associated with disastrous landslides.

# 1. Introduction

The Southeast region of Brazil has been historically impacted by heavy rainfall due to the influence of several weather systems, such as the Cold Front (CF) and the South Atlantic Convergence Zone (SACZ) (Lima et al., 2010). In Rio de Janeiro state, the combination of the proximity to the coast and rugged terrain generates a high precipitation spatial variability with several areas being impacted by extreme rainfall

https://doi.org/10.1016/j.wace.2025.100811

Received 19 September 2023; Received in revised form 30 September 2025; Accepted 30 September 2025 Available online 11 October 2025

2212-0947/Crown Copyright © 2025 Published by Elsevier B.V. This is an open access article under the Open Government License (OGL) (http://www.nationalarchives.gov.uk/doc/open-government-licence/version/3/).

<sup>\*</sup> Corresponding author. Engineering Science, University of Oxford, Oxford, UK. E-mail address: sarah.sparrow@oerc.ox.ac.uk (S. Sparrow).

events, particularly over the Serrana region (Rio de Janeiro mountain area), the Sul Fluminense (Southern part of Rio de Janeiro state) and the Rio de Janeiro Metropolitan Area (Lima et al., 2021).

Among the consequences of heavy rainfall, floods and landslides are the most impactful phenomena in Brazil. It is estimated that 37 % of all South America landslides are concentrated in Brazil, mainly in the South and Southeast regions (Dias et al., 2021), and were responsible for 74 % of the deaths related to disasters between 1991 and 2010 (Debortoli et al., 2017). The increase in precipitation extremes can amplify the risk of landslides through soil infiltration, soil erosion, and an increase in surface runoff (Gariano and Guzzetti, 2016); however, there is still uncertainty in quantifying the impact of climate change on landslide occurrences due to a lack of records and sparsity of studies across the globe. Moreover, with increased greenhouse gas emissions, it is estimated that there is a significant increase in Brazil's susceptibility to landslides and flash floods. Notably, regions already considered to have high susceptibility, such as the mountainous region of Rio de Janeiro, are projected to become even riskier by the end of the century (Debortoli et al., 2017). The most impactful disaster related to landslides in the country occurred in this mountainous region of Rio de Janeiro state in 2011, resulting in approximately 947 deaths, mainly in the municipalities of Nova Friburgo, Teresópolis, and Petrópolis (Dourado et al.,

Given the increasing frequency and severity of these extreme events, especially in densely populated and vulnerable areas, it has become essential to understand the extent to which they may be influenced by anthropogenic climate change. Attribution studies aim to assess the extent to which the likelihood of these extreme events can be attributed to anthropogenic climate change, to identify the influence of human activities on their occurrence (Hegerl et al., 2010). Event attribution has developed rapidly in the last decade due to the demand for explaining the increased probability and magnitude of extreme events (Stott et al., 2016). For example, Otto et al. (2015) studied the water crisis that occurred in Central-Southern Brazil between 2014 and 2015. The authors found that this extreme event could not be significantly attributed to anthropogenic forcing, with the vulnerability being the most relevant factor instead. On the other hand, Dalagnol et al. (2022) showed that the extreme precipitation that occurred in Minas Gerais, Brazil, in January 2020 was, at least, 70 % more likely to happen due to human-induced climate change, and 41 % of the financial impacts also could be attributed to climate change. Attribution analysis has also been developed for other events such as heatwaves (Leach et al., 2021; Wang and Wang, 2023), extreme temperatures and droughts (Wang et al., 2017, 2018; Neto et al., 2021), and floods (Hirabayashi et al., 2021; Kundzewicz and Pińskwar, 2022; Quevedo et al., 2025). These studies are particularly important and timely because under the Brazilian Federal Law 14.904 from June 2024, associated with the National Fire Management Plan, it has been demanded the development of climate change adaptation plans at different scales, from local, municipal, state and federal levels. In order to develop realistic and useful plans, the identification, assessment and understanding of the vulnerability and exposure of environmental, social, economic and infrastructure systems to extreme events and how they are changing is key.

Petrópolis was again hit by a devastating disaster in February 2022, when the meteorological station data in the municipality recorded 252.8 mm within 3 h (Alcântara et al., 2023), leading to landslides that reached a total area of 37 km² (Netto et al., 2022). Two days before the tragedy, the National Centre for Monitoring and Alerting Natural Disasters (CEMADEN) issued an alert of an upcoming very intense meteorological event. However, despite this warning, 78 people died (with unofficial estimates exceeding 200 people) and hundreds more were displaced or left homeless in what is now registered as the deadliest disaster in the municipality (FIDE, 16/02/2022).

In this context, the main objective of this study is to investigate the extreme rainfall event that triggered numerous landslides in Petrópolis, Brazil, in February 2022. The study integrates event attribution and

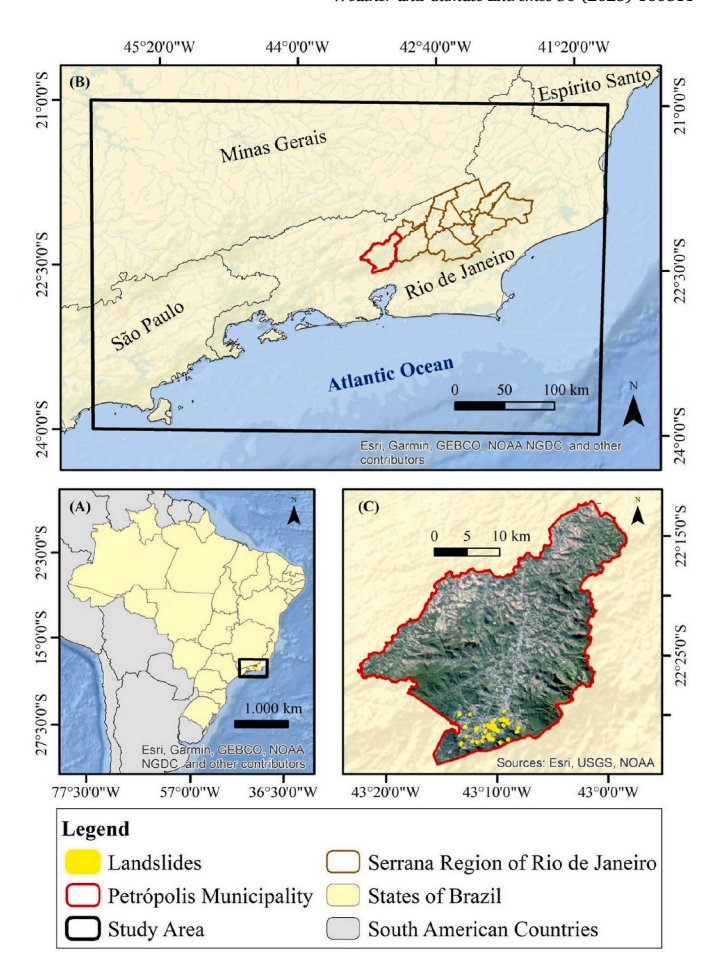


Fig. 1. Study area. A) Location of the study area in Brazil; B) Polygon area for analyzing the extreme precipitation event; C) Petrópolis municipality and landslide occurrence.

impact assessment to evaluate both the climatic and socioeconomic dimensions of the disaster. Specifically, we address the following research questions: (1) How much of the heavy rainfall event can be attributed to anthropogenic climate change? (2) How do changes in Land Use and Land Cover (LUCC) contribute to the region's landslide susceptibility? and (3) What socioeconomic impacts are related to the 2022 landslide disaster?

# 2. Methodology

## 2.1. Study area

Our study focused on the extreme rainfall event that occurred in February 2022, which triggered several landslides in the Petrópolis municipality, located in the mountainous region of Rio de Janeiro, Southeast Brazil. For the rainfall event analysis, we considered a polygon area with the following coordinates:  $21^{\circ}0'0''$  S and  $41^{\circ}0'0''$  W;  $24^{\circ}0'0''$  S and  $46^{\circ}0'0''$  W. The selected area comprises nearly the entire Rio de Janeiro state and part of São Paulo, Minas Gerais, and Espírito Santo states (Fig. 1). This area covers approximately 171,000 km², large enough to be analyzed with global satellite and climate model precipitation data.

The analyzed area is composed of a mountainous relief known as the Serra do Mar, a system of escarpments and mountains that began to form during the Cretaceous period (90 Ma). The specific geomorphological characteristics result from the lithological differences due to formative morphotectonic events, as well as the complex fault systems and shear zones (Vieira and Gramani, 2015). Furthermore, the proximity of these

mountains to the coast influences the rainfall spatial distribution. The study area is characterized by the Atlantic Forest biome, with the presence of a dense ombrophilous forest.

Currently integrated into the Metropolitan Region of Rio de Janeiro (IBGE – Instituto Brasileiro de Geografia e Estatística, 2025), Petrópolis is located near major urban centers, including the state capital. Recognized for its historical and urban significance, Petrópolis was one of the first planned cities in Brazil, with its initial occupation delimited by the Köeler Plan. However, throughout the 19th and 20th centuries, economic and demographic transformations, particularly driven by industrialization, led to a significant urban expansion beyond the boundaries originally established (Ambrozio, 2008). This unregulated growth, combined with the scarcity of adequate land for urban infrastructure, resulted in the occupation of hillside and ridge areas, characterized by steep terrain and high environmental fragility.

From the 1970s onwards, the abandonment of the Köeler Plan and the lack of effective urban planning led to deforestation, precarious settlements, inadequate sanitation infrastructure, and an intensification of floods and landslides (Guerra et al., 2007; Antunes and Fernandes, 2020; Costa et al., 2022). It is estimated that around 24 % of the municipal population, approximately 72,000 people, are currently exposed to landslide and flood risks (de Assis et al., 2018). This socioenvironmental vulnerability is further exacerbated by the municipality's location within the Serra do Mar Mountain range in the state of Rio de Janeiro, a region heavily influenced by atmospheric systems such as the South Atlantic Convergence Zone (SACZ) and cold fronts, which have historically contributed to the occurrence of extreme rainfall events (Tavares and Ferreira, 2020; Costa et al., 2022).

In addition to these socio-environmental challenges, Petrópolis also stands out for its historical and contemporary role as a major tourist destination. Considered one of Brazil's first tourist destinations, the municipality has recently established itself as one of the main attractions in the state of Rio de Janeiro. Tourism accounts for approximately 6 % of the municipality's annual GDP, equivalent to over U\$141.07 million<sup>2</sup> (Câmara Municipal de Petrópolis, 2022), and in 2019 alone, the city received around two million visitors (Prefeitura, 2019). This economic dynamism is also reflected in indicators such as its high Human Development Index (0.745) and one of the highest Gross Domestic Products in the region (IBGE – Instituto Brasileiro de Geografia e Estatística, 2025).

Given this context, the combination of unplanned urban growth and the natural configuration of the territory makes Petrópolis highly susceptible to floods, flash floods, and landslides-vulnerabilities that stand in contrast to its economic and touristic importance. In 2011, extreme rainfall and consecutive landslides affected this region, encompassing 23 municipalities (Cardozo and Monteiro, 2019) and impacting over 7,000 people (Rosi et al., 2019). Among the affected municipalities, Petrópolis was one of the most impacted and again experienced severe losses from landslides and flooding in February 2022. In this sense, assessing the influence of anthropogenic climate change on the extreme rainfall event, along with the analysis of its socioeconomic impacts in Petrópolis, provides a diagnosis of how these factors have contributed to increasing social vulnerability. This scenario highlights the urgent need for greater investment in adaptation strategies and land use planning to reduce disaster risk, especially in the face of significant economic losses resulting from a recurring cycle of large-scale disasters.

# 2.2. Data

#### 2.2.1. Observational rainfall data and climate models

Daily rainfall data from 177 pluviometric stations, provided by

CEMADEN, were used to characterize the event both temporally and spatially. The data, available from 2000 onward, included stations located in Petrópolis (considered main stations) as well as in neighboring municipalities (complementary stations), covering a total of 26 municipalities. The goal was to assess the rainfall distribution on the day of the extreme event in the mountainous central region of the state of Rio de Janeiro.

Additionally, we used the CPC Global Unified Gauge-Based Analysis of Daily Precipitation data at 0.5° spatial resolution (Chen et al., 2008) as the gridded observational dataset. This dataset is available from 1979 onwards and was resampled to N216 spatial resolution to match the climate model used in our analysis. The CPC dataset has been previously used in research focused on tropical regions (Solman and Blázquez, 2019; Dalagnol et al., 2022), and provides sufficiently accurate estimates to study tropical rainfall patterns.

For the attribution analysis, we used the global climate model Hadley Centre Global Environmental Model version 3-A (HadGEM3-A). This global climate model is part of the HadGEM family and is based on the HadGEM3 atmospheric component, which is operated at a N216 horizontal resolution with 85 vertical levels (Davies et al., 2005; Ciavarella et al., 2018). The model simulations used for the attribution analysis consist of one experiment considering natural-only forcing from volcanic activity and solar variability ("NAT"), while keeping all other forcings constant at 1850 levels, and a second experiment considering both natural and anthropogenic forcings combined ("ALL"). For the year 2022, 525 ensemble members are available for each experiment, creating a large ensemble for the attribution analysis, as part of the extended ensemble. In contrast, for the historical period (1981-2013), the model includes 15 ensemble members (Ciavarella et al., 2018; Dalagnol et al., 2022). A more comprehensive description of the attribution system using the HadGEM3-GA6 model can be found at Ciavarella et al. (2018) and Vautard et al. (2019).

#### 2.2.2. Land use and land cover change (LUCC)

For the LUCC analysis, we used data from collection 10 of the MapBiomas project (https://mapbiomas.org/en). MapBiomas is a collaborative and open-source monitoring initiative founded in 2015 to address the land use and land cover (LULC) information gap in Brazil and monitors transformations in the Brazilian territory (Souza Jr et al., 2020). MapBiomas facilitates collaboration with a network of non-governmental organizations, universities, and private companies. The annual LULC mapping with 30 m spatial resolution from 1985 to 2024. In this study, we assessed the LUCC up to 2022 and analyzed their trends. We also analyzed the LUCC in hilltops, aiming to identify possible relationships with landslide occurrence. To identify the hilltops, we used the Digital Elevation Model (DEM) from the Shuttle Radar Topography Mission (SRTM), selecting the SRTM 1 Arc-Second Global with 30 m spatial resolution obtained from the Google Earth Engine (GEE) platform (Farr et al., 2007).

# 2.2.3. Socioeconomic impacts database

We obtained the socioeconomic impacts from the Integrated Disaster Information System (S2ID, 2024). The S2ID is the official platform for disaster information in Brazil and contains data on location (municipality), type of disaster, date and time of occurrence, causes and effects, human and material damage, and public and private economic losses. The local civil defense collects and registers this information in the S2ID within 10-15 days after the declaration of an emergency, aiming to get financial resources from the federal government for disaster relief (BRASIL. Instrução Normativa  $N^\circ$  36 de 4 de dezembro de, 2020).

# 2.3. Method

# 2.3.1. Extreme rainfall attribution

The CPC observational data were used to define the extreme rainfall event threshold used in the attribution study. Based on prior assessment

<sup>&</sup>lt;sup>1</sup> The Köeler Plan, developed by engineer Júlio Frederico Köeler, was an urbanization project that defined the initial urban core of Petrópolis (Soares, 2009; Costa et al., 2022).

of the most-affected areas, we selected the austral summer of 2021-2022 (December, January, and February) as our study period, which is the peak rainy season in Southeast Brazil. The study focused on the spatial maximum of accumulated rainfall over 3-day (Rx3day), 30-day (Rx30day), and 60-day (Rx60day) periods within the study area, adopted as representative metrics of rainfall intensity. The spatial maximum was determined by aggregating rainfall over these specific metrics (3, 30, and 60 days) and subsequently identifying the highest value across the spatial region. Several tests were run to determine the most suitable metrics that could be consistently applied to both model and observational data and still represent the observed event. We chose three different metrics to evaluate the rainfall conditions around the time of the event (Rx3day), which may represent the short-term precipitation that triggered the landslide, and also before the event (Rx30day and Rx60day) to understand the influence of antecedent conditions, which increase soil moisture and therefore susceptibility, on

A climatological reference period of 1981–2013 was used for model validation, in line with the 30 years commonly used to analyze long-term climate data, as well as being a common period available between observations and model data. We obtained histograms to analyze the differences between the CPC dataset and the HadGEM3-A ensemble models and identify model biases. To correct the bias, we normalized the data by the climatology, applying the following equation to the CPC and HadGEM3-A datasets for the three selected metrics:

$$\frac{Rx_{n-day}}{X_{climatological}}$$
 Equation (1)

where Rx represents the maximum cumulative precipitation for each n-day (3-day, 30-day, and 60-day) and X is the historic mean based on the climatology (1981–2013). The equation was applied for both CPC and HadGEM3-A datasets, separately.

Based on the normalization of the datasets (bias correction), the Generalized Extreme Value (GEV) distribution was fitted to the data. Following this adjustment, the Probability Ratio (PR) was calculated to quantify how much more likely it is to exceed the CPC-observed precipitation threshold in the ALL scenario compared to the NAT scenario. The PR is defined as the ratio between the probability (P) of exceeding the CPC threshold in the ALL scenario and the probability of exceeding the same threshold in the NAT scenario. Confidence intervals were also estimated (Equation (2)). This step was performed for the three selected rainfall metrics.

$$PR = \frac{P_{ALL}}{P_{NAT}}$$
 Equation (2)

We also calculated the Attributable Risk Fraction (FAR), which corresponds to the fraction that can be attributed to climate change (Allen, 2003). FAR can be used to estimate the proportion of the damage caused by human-induced climate change (Stott et al., 2016; Quevedo et al., 2025). It is a measure of the contribution of anthropogenic forcing to the occurrence or severity of the extreme event (Stott et al., 2004; Otto et al., 2016; Otto, 2017; Frame et al., 2020; Dalagnol et al., 2022). Although FAR may not precisely represent the risk attributable to anthropogenic climate change, especially in contexts where the relationships between meteorological variables and impacts are non-linear (Perkins-Kirkpatrick et al., 2022), FAR remains a valuable metric by providing an initial estimate of this contribution. This is particularly relevant in situations where such relationships are complex and there is no clear transfer function between the meteorological event and the observed impacts (Carlson et al., 2024), as is the case in this study. To calculate the FAR, we used the following equation:

$$FAR = 1 - \left(\frac{1}{PR}\right)$$
 Equation (3)

We calculate the return period based on the inverse of the probability

**Table 1**- Reclassification of original MapBiomas Collection 10 classes into nine analytical categories.

New Class	Original MapBiomas C10 Categories		
1 – Forest formation	Forest Formation (1)		
2 - Forest Plantation	Forest Plantation (50)		
3 - Herbaceous and	Herbaceous and Shrubby Vegetation (10), Grassland		
Shrubby vegetation	Formation (11), Hypersaline Tidal Flat (12), Rocky		
	Outcrop (29), Herbaceous Sandbank (32) Whetland		
3 - Other forest types	Savanna Formation (4), Mangrove (5), Floodable		
	Forest (6), Wooded Sandbank (49)		
4 – Pasture	Pasture (15)		
5 – Temporary Crops	Agriculture (19), Soybean (20), Sugarcane (39), Rice		
	(40), Cotton (41)		
6 – Perennial Crops	Coffee (35), Citrus (36), Oil Palm (46), Other		
	Perennial Crops (47), Perennial Crop (48)		
7 – Urban	Urban Area (22)		
8 – Water	Water Body (26), River/Lake/Ocean (31),		
	Aquaculture (33)		
9 – Other	All remaining categories are not included in the		
	groups above		

of exceeding the threshold for each of the scenarios using the 525 ensemble members to compute the probabilities. We also estimated the probability ratio based on a two-dimensional probability analysis, where we consider both the short-term trigger (Rx3day) and the long-term antecedent conditions (Rx60day). This means that we want to find how climate change affects the probability of an event happening where we have larger values of precipitation before the event, building soil moisture, and intense precipitation right before the event, triggering the landslide.

#### 2.3.2. LUCC evaluation

2.3.2.1. Reclassification. The LULC data were obtained from MapBiomas Collection 10, available on GEE platform. For the municipality of Petrópolis, the original classification system, which includes more than seventy categories, was reclassified into nine broader classes to facilitate the analysis and ensure comparability over time. The reclassification grouped the categories into forest, other forest types, natural vegetation, pasture, temporary crops, perennial crops, urban areas, water bodies, and others (Table 1). The annual maps from 1985 to 2024 were clipped to the municipal boundaries and subsequently harmonized into this reduced classification. This methodological step enabled a consistent assessment of land use and land cover dynamics across the study period.

# Detection of hill tops of Permanent Preservation Areas (APPs)

The Brazilian Forest Code (Law n° 12,651 of 2012) defines hilltops as APPs when: (i) the total elevation difference (amplitude) from base to summit is greater than 100 m, (ii) the average slope exceeds 25°, and (iii) the upper third portion of the hill meets these two conditions. Additionally, all areas above 1,800 m in elevation must be preserved, regardless of vegetation type. These areas are key for mitigating landslide risks (Cohen and Schwarz, 2017; Lehmann et al., 2019). To identify APP-eligible hilltops not currently protected, we used a Hydrologically Consistent Digital Elevation Model (HCDEM) to correct depressions and generate a continuous elevation surface. From this, we derived slope and elevation maps (Pereira et al., 2014). The method included:

- Hilltop delimitation: Identification of individual topographic highs (summits) using elevation inversion and flow accumulation to delineate hill massifs.
- Slope analysis: Calculation of the average slope
- <u>S</u> for each hilltop:

$$\underline{S} = \frac{1}{n} \sum_{i=1}^{n} Si$$
 Equation (4)

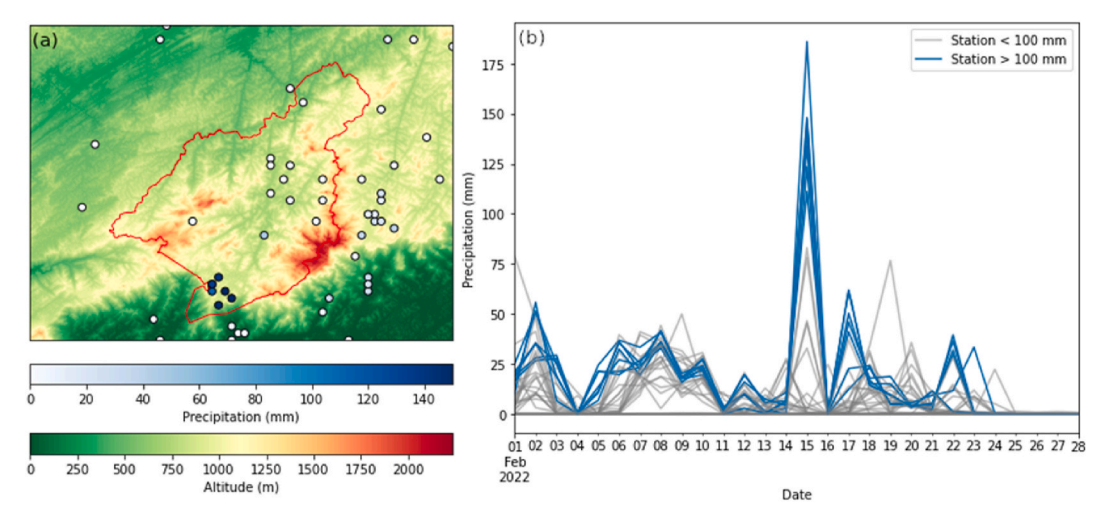


Fig. 2. Extreme Rainfall Event Characterization. (a) Spatial distribution of accumulated precipitation (mm) on February 15 for the weather stations available in the area. The red line highlights the city of Petrópolis, the shaded colors are the altitude in meters, and the markers are the available weather stations colored according to the precipitation; (b) Time Series of daily accumulated precipitation for February 2022 for the available weather stations in the area.

where  $S_i$  is the slope (in degrees) of each pixel, and n is the number of pixels in the hilltop area.

- Elevation amplitude: Computation of total elevation range:

$$A = H_{max} - H_{min}$$
 Equation (5)

where  $H_{max}$  and  $H_{min}$  are the maximum and minimum elevations within the hilltop unit.

 Upper third identification: Definition of the upper third elevation band:

$$H_{upper\ third} = H_{max} - \frac{A}{3}$$
 Equation (6)

All pixels with elevation  $\geq H_{upper third}$  and located on hills with A  $\geq$  100m and  $\underline{S} \geq$  0.25° were flagged as APP-eligible hilltops.

2.3.2.2. Trend analysis. To analyze LULC dynamics within hilltop APPs in the municipality of Petrópolis, a Bayesian hierarchical regression model (Schmid et al., 2000; Seltzer et al., 1996) was applied. Annual data on the area occupied by each LULC class from 1985 to 2024 were organized as a time series, considering seven aggregated categories: forest, other forest types, natural vegetation, pasture, temporary crops, perennial crops, and urban areas.

The model assumes that, for each class j and year t, the observed area  $Y_{t,j}$  follows a normal distribution:

$$Y_{tj} \sim N\left(\mu_{t,i}, \sigma_j^2\right)$$
 Equation (7)

Where the expected value  $\mu_{t,i}$  is modeled as a linear function of time:

$$\mu_{t,j} = \alpha_j + \beta_j * (t - \underline{t})$$
 Equation (8)

Here,  $\alpha_j$  is the intercept,  $\beta_j$  is the slope representing the temporal trend, and (t-t) denotes the centered year to improve model convergence. The prior distributions were specified as weakly informative to allow flexibility while regularizing estimates:

$$\alpha_i \sim N(0, 100^2), \beta_i \sim N(0, 10^2), \sigma_i \sim HalfNormal(50)$$

Posterior distributions of the parameters  $\alpha_j$ ,  $\beta_j$  and  $\sigma_j$  were estimated using Markov Chain Monte Carlo (MCMC) (Karandikar, 2006; Zobitz et a.,l 2011; Nemeth et al., 2021) with the No-U-Turn Sampler (NUTS) algorithm (Nishio and Arakawa, 2019; Alawamy et al., 2022). From the posterior estimates, the expected temporal trajectories of each land use

class were reconstructed, including 95 % credible intervals:

$$\hat{Y}_{t,j} \pm 1.96 * SD(Y_{t,j}^{posterior})$$
 Equation (9)

These trajectories provided a probabilistic quantification of longterm trends in LUCC categories, enabling robust inferences on land use transitions within environmentally sensitive areas.

2.3.2.3. Association with landslide areas. To elucidate the relationship between land use dynamics and landslide occurrences, a comprehensive dataset of landslide locations within the municipality of Petrópolis was compiled. For each location, the corresponding LULC class was extracted for the years 1985, 2012, and 2022, enabling a detailed assessment of land cover transitions over time in landslide susceptible areas. The aggregate area occupied by natural vegetation, comprising forest, other forest types, and natural vegetation classes, was computed for each point, and the magnitude of vegetation loss between consecutive periods (1985–2012 and 2012 to 2022) was quantified.

Transition matrices were generated to quantify the number of points transitioning between LULC classes during each temporal interval, providing a nuanced depiction of LUCC dynamics within landslide-prone areas. Furthermore, relative landslide risk was estimated for each class as the proportion of points experiencing landslides relative to the total number of points classified within that category. To visually represent these dynamics, Sankey diagrams were employed, in which nodes correspond to LULC classes at each time point, and links denote the number of points undergoing transitions between classes. Node colors were assigned according to LULC categories, while link colors incorporated partial transparency to emphasize predominant transitions without obscuring minor flows.

#### 2.3.3. Socioeconomic damages estimation

The socioeconomic impacts of the extreme precipitation event in Petrópolis (February 2022) were assessed using official data from the S2iD and complementary municipal and state government sources. The analysis was structured into two main components: human impacts and economic impacts, both categorized and tabulated for clarity and crossverification. Human impacts were analyzed based on the officially reported number of individuals affected, including those injured, displaced, left homeless, or deceased. These figures were extracted from the first official damage assessment (FIDE, 16/02/2022), which reflects data collected within the first 24 h after the event. It is important to note that this initial assessment likely underestimates the total human toll, as the municipal civil defense later reported at least 240 fatalities through

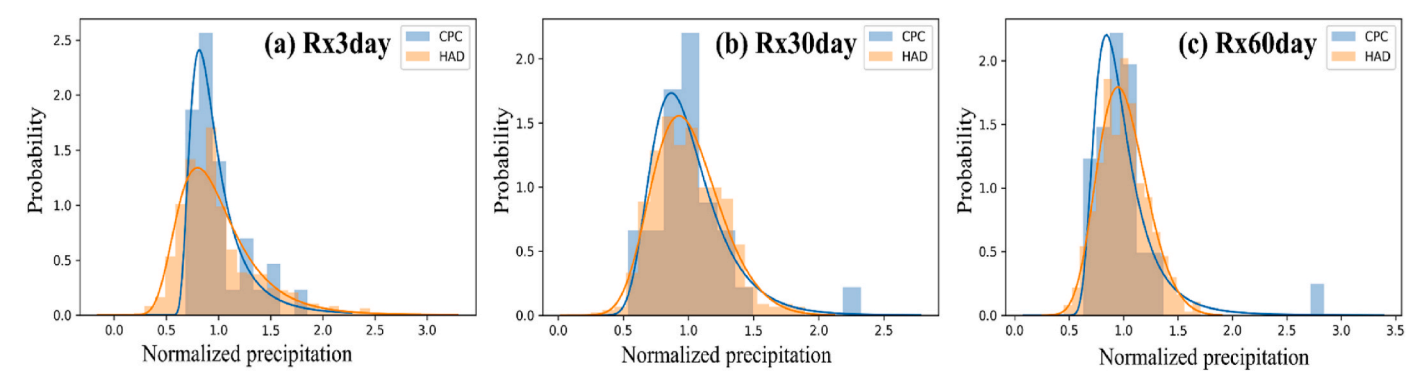


Fig. 3. Histograms of bias-corrected CPC and the HadGEM3-A model for the spatial maximum of the (a) Rx3day, (b) Rx30day, and (c) Rx60day.

media channels. Moreover, no estimates were available for the indirectly affected population, which may be substantially higher than those directly impacted.

Economic impacts were calculated based on official estimates of losses and damages, converted from Brazilian reais (BRL) to United States dollars (USD) using the average exchange rate for the year of the event, as published by the Central Bank of Brazil (1 USD = 5.16 BRL). The losses were classified into three categories: 1. Private economic losses, primarily in the commerce/services and agriculture sectors, 2. Public economic losses, including damages to urban cleaning services, water supply, sewage, and healthcare infrastructure, and 3. Material damages, notably to public infrastructure and private dwellings.

All monetary values were compiled into structured tables and cross-verified with multiple governmental sources to ensure consistency and accuracy. This disaggregation enabled the identification of the most affected sectors and the proportional contribution of each loss category to the total economic impact. Data limitations and uncertainties were considered, especially regarding the temporal scope of data collection and the unavailability of updated figures on long-term impacts.

# 3. Results

# 3.1. Event definition

The extreme precipitation event on February 15 was concentrated in the southern portion of Petrópolis (Fig. 2), with accumulations exceeding 100 mm. Petrópolis—a municipality in the state of Rio de Janeiro situated in a high-relief area—has the windward slope of the mountain range in its southern section, which is precisely where rainfall was concentrated. The rest of the municipality and neighboring towns recorded low totals, between 0 and 40 mm. Moreover, the 15th was the

only and most intense precipitation peak of the month, underscoring the event's highly concentrated nature in both space and time at the scales analyzed.

#### 3.2. Model validation

To validate the HadGEM3-A model, we compared the modeled precipitation with the observational CPC data from 1981 to 2013. We found a positive model bias of approximately 90, 160, and 245 mm for Rx3day, Rx30day, and Rx60day, respectively, indicating an overestimation of the precipitation metrics by the HadGEM3-A. After the bias correction and application of the GEV distribution (Fig. 3), the two datasets significantly increased their overlap, especially for the Rx30day and Rx60day metrics, and the bias was reduced to almost zero. These results indicate that the HadGEM3-A can satisfactorily be used in our study area. However, we should notice that CPC indicates a few events in the right tail of the distribution for Rx30day and Rx60day, which are not present in the model, and might indicate that the model is not good at capturing such extreme events.

# 3.3. Attribution analysis

We used ALL and NAT scenarios from HadGEM3-A to compute the changes in likelihood of the event (Fig. 4). The distributions for the three metrics (RX3day, RX30day, and RX60day) were all slightly shifted to the right under the ALL scenario, suggesting higher precipitation values are expected when considering human-induced climate change (Fig. 4). Notably, the CPC precipitation threshold for the Rx60-day is also located further right in the graph (Fig. 4c). This suggests that such extreme rainfall events are relatively rare in both scenarios (ALL and NAT) but become more probable to occur under human-induced climate change.

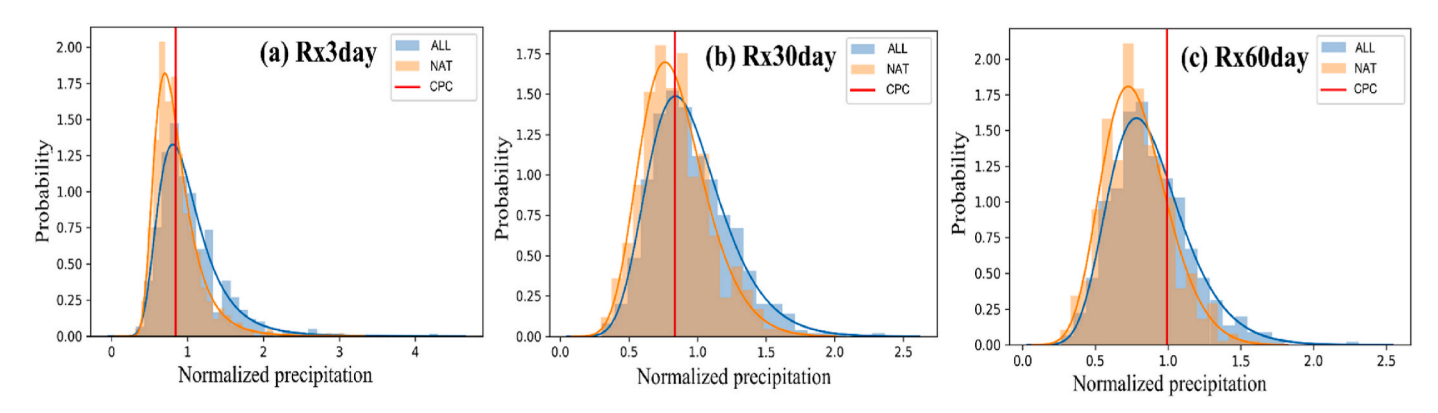


Fig. 4. Histograms and GEV fitted distributions of the spatial maximum for the three metrics, (a) RX3day, (b) RX30day, and (c) RX60day, for ALL (blue) and NAT (orange) scenarios from the HadGEM3-A model using CPC climatology for bias model correction. The thresholds from CPC for exceedance probability calculation in each case are shown in the red line.

Table 2

Attribution metrics for the extreme precipitation event in Câmara Municipal de Petrópolis, 2022), based on the ALL and NAT scenarios, using the CPC observed threshold. Probabilities and return periods were calculated using the fitted GEV distribution. The 95 % confidence interval (CI) was obtained by the 2.5th and 97.5th percentiles using 1 000 bootstrap simulations. For the event threshold, we show the value in millimeters and normalized by the 1981–2013 average.

Metric	Rx3day Estimate [95 % CI]	Rx30day Estimate [95 % CI]	Rx60day Estimate [95 % CI]
Event threshold	118.16 mm	399.15 mm	763.34 mm
(mm)	(0.84)	(0.84)	(0.99)
Probability Ratio	1.45 [1.31,	1.30 [1.18, 1.44]	1.71 [1.42, 2.05]
(PR)	1.60]		
Attributable Risk	0.31 [0.24,	0.23 [0.15, 0.31]	0.41 [0.29, 0.51]
Fraction (FAR)	0.38]		
ALL Return period	1.63 [1.54,	1.63 [1.54, 1.73]	3.31 [2.97, 3.72]
(years)	1.72]		
NAT Return period	2.36 [2.18,	2.13 [1.97, 2.30]	5.66 [4.94, 6.67]
(years)	2.59]		

On the other hand, the Rx3day and Rx30day CPC thresholds remained near the distribution mean for both scenarios, suggesting that maximum rainfall accumulations of this magnitude over these timescales are more typical, i.e., less extreme.

The event thresholds for the Rx3day, Rx30day, and Rx60day were 118.16 mm, 399.15 mm, and 763.34 mm, respectively (Table 2). All calculated PR were greater than one, indicating that anthropogenic climate change has increased the likelihood of rainfall events above the calculated thresholds. This increase is statistically significant at the 5 % confidence level. The PR for the Rx3day and Rx30day were similar and characterized by lower PR (1.45 and 1.30, respectively) when compared to the Rx60day (1.71). These results indicate an increase of 45 % in the likelihood of short-term extreme rainfall events (Rx3day) occurring, which are commonly associated with landslide triggers, and a 71 % increase for the long-term rainfall events (Rx60day), highlighting the influence of antecedent conditions in landslide susceptibility.

The FAR results similarly show that the damage caused by this event can be attributed to anthropogenic climate change by 31 % (0.31) for the Rx3day, 23 % (0.23) for Rx30day, and 41 % (0.41) for Rx60day. Despite FAR having limitations, as it may not always express the non-linear relations between the hazard and the impact, it is a first estimate of the attributable damage when we have complex relationships that are not easily modeled (Perkins-Kirkpatrick et al., 2022; Carlson et al., 2024). Furthermore, the return period indicates that in the ALL scenario (considering anthropogenic climate change), the recurrence of an event of this type would increase. While in the NAT scenario (natural forcing

only), the return period is around 2.4-5.6 years, in ALL, this period is 1.6-3.3 years.

The comparison between the Rx3day and Rx60day (Fig. 5) demonstrated that the density of points exceeding both the Rx3day and Rx60day thresholds is higher in ALL than in NAT. To quantify whether the difference between ALL and NAT was significant, we calculated the PR accounting for the number of members above the threshold. The PR value is 2.06 [1.46, 2.30], demonstrating that the probability of the event in the Rx3day and Rx60day metrics in the climate change scenario is approximately twice as high as in the natural scenario. We also calculated the PR using a conditional probability, where the calculated PR was conditioned on both Rx3day and Rx60day being higher than the CPC threshold, instead of just one of them, as in Fig. 4, getting a value of 1.46 [1.17, 1.88].

#### 3.4. LUCC analysis

#### 3.4.1. Land use change in hill tops from 1985 to 2024

The analysis of average annual variation by period (Fig. 6a and Table 3) reveals distinct dynamics across land cover categories in Hilltop APPs. The "Pasture" land cover class consistently shows the highest average annual losses, with a marked decline of -2.17 % during the period 2015–2024, reinforcing its role as the main source of land-use conversion. In contrast, "Urban" areas exhibit the most consistent gains throughout the study period, peaking at 4.43 % per year in 1985–1994 and remaining positive thereafter, though at lower rates (1.18 % per year in 2015–2024).

Among forest-related categories, "Forest Formation" maintains small but steady positive growth across all periods, ranging from 0.19 % to 0.67 % per year, while "Forest Plantation" records a sharp increase only in the most recent period (6.98 % per year in 2015–2024). "Herbaceous/ Shrubby Vegetation" alternates between modest positive changes in earlier decades (0.56–0.72 % per year) and losses in 2015–2024 (-0.48 % per year). "Other Forest Types" remain stable, with no significant changes across periods.

Agricultural classes (Temporary and Perennial Crops) show negligible average variations close to zero, suggesting limited expansion or contraction. Water and "Other" categories, on the other hand, display substantial fluctuations: "Water" registers losses in 1985–1994 ( $-0.20\,$ % per year) and 1995–2014 (-1.44 to  $-1.63\,$ % per year), followed by a small recovery in 2015–2024 (0.35 $\,$ % per year). The "Other" class, which likely aggregates transitional or undefined covers, presents high volatility, with a major reduction in 1985–1994 ( $-9.20\,$ % per year), subsequent recovery in 1995–2004 (4.07 $\,$ % per year), and minor oscillations in later periods.

Fig. 6b, which illustrates annual variation in absolute area (km<sup>2</sup>),

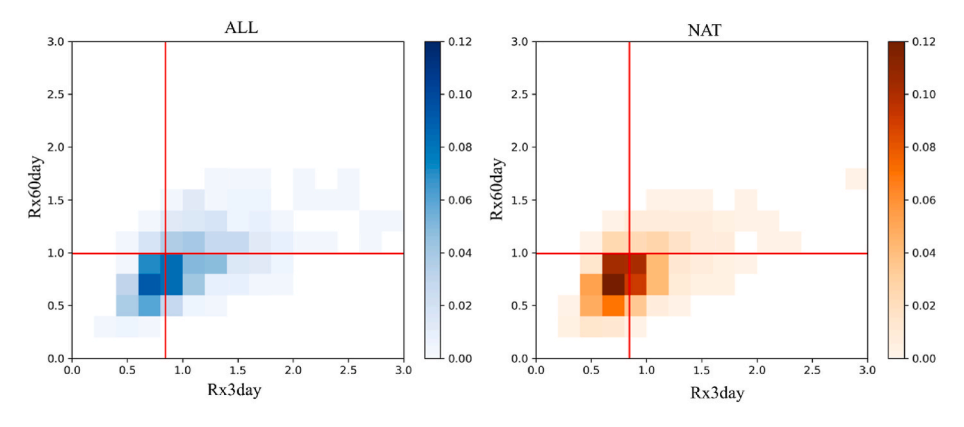
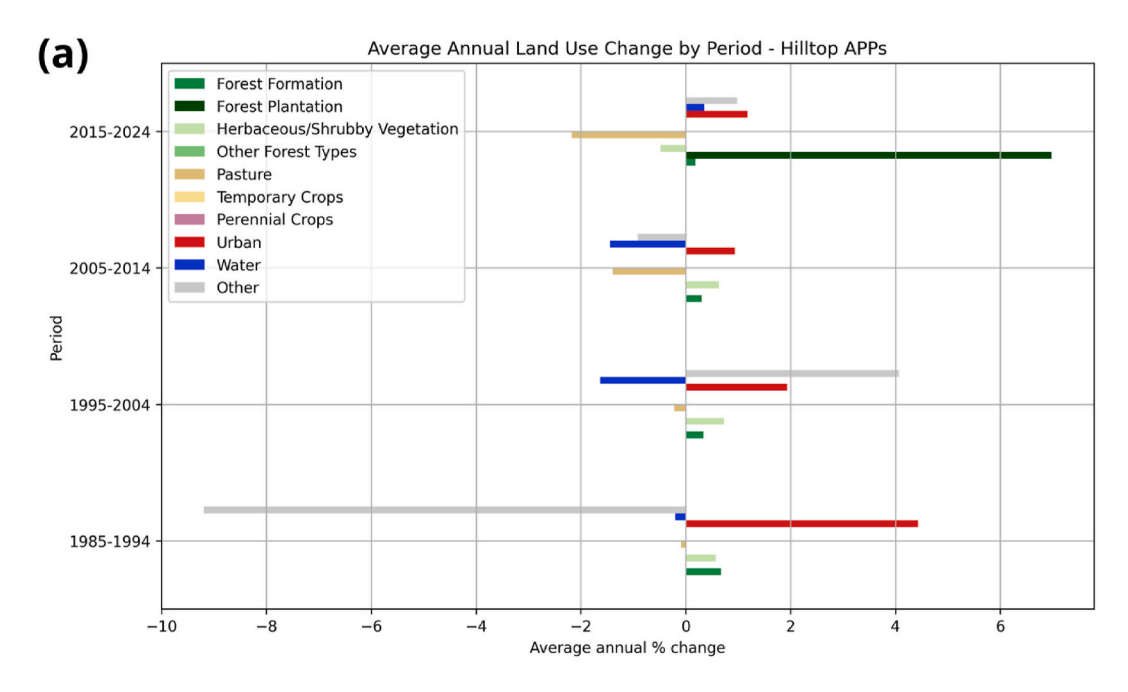
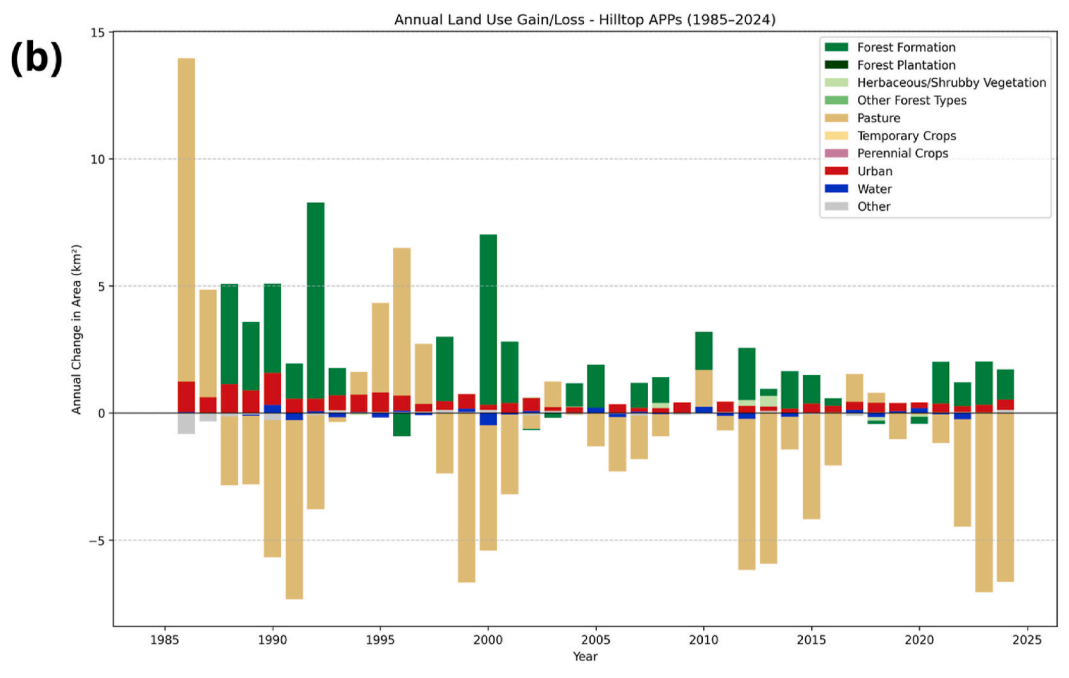


Fig. 5. Joint density histogram of ensemble members for the maximum values of short-term (Rx3day) and long-term (Rx60day) precipitation metrics under the ALL (left) and NAT (right) scenarios from the HadGEM3-A model. Colors represent the probability density of event occurrence in each grid cell, with blue tones for the ALL scenario and orange to red tones for the NAT scenario. Red lines indicate the observed precipitation thresholds on the event day, based on CPC data, for both Rx3day and Rx60day metrics. All values are normalized with respect to the 1981–2013 climatology.





**Fig. 6.** Land use and land cover (LULC) dynamics within hilltop permanent preservation areas (APPs) in Petrópolis between 1985 and 2024; (a) Average annual percentage change of land use classes by period (1985–1994, 1995–2004, 2005–2014, and 2015–2024) and (b) Annual net gain and loss in area (km<sup>21</sup>) of land use classes for the entire period of analysis (1985–2024).

Table 3

Average annual percentage change of land use and land cover (LUCC) classes in hilltop APPs, Petrópolis, 1985–2024.

Period	Forest Formation	Forest Plantation	Herbaceous/Shrubby Vegetation	Other Forest Types	Pasture	Temporary Crops	Perennial Crops	Urban	Water	Other
1985–1994	0.67	0.00	0.56	0.00	-0.09	0.00	0.00	4.43	-0.20	-9.20
1995-2004	0.33	0.00	0.72	0.00	-0.22	0.00	0.00	1.93	-1.63	4.07
2005-2014	0.30	0.00	0.63	0.00	-1.39	0.00	0.00	0.94	-1.44	-0.92
2015-2024	0.19	6.98	-0.48	0.00	-2.17	0.00	0.00	1.18	0.35	0.98

highlights strong interannual variability, especially for pastures, which alternate between pronounced gains and losses over the decades. In the late 1990s and early 2000s, pasture losses were particularly intense,

while earlier years occasionally recorded gains. Urban expansion appears as a persistent upward trend, though less variable than pasture dynamics. Forest Formation and Herbaceous/Shrubby Vegetation

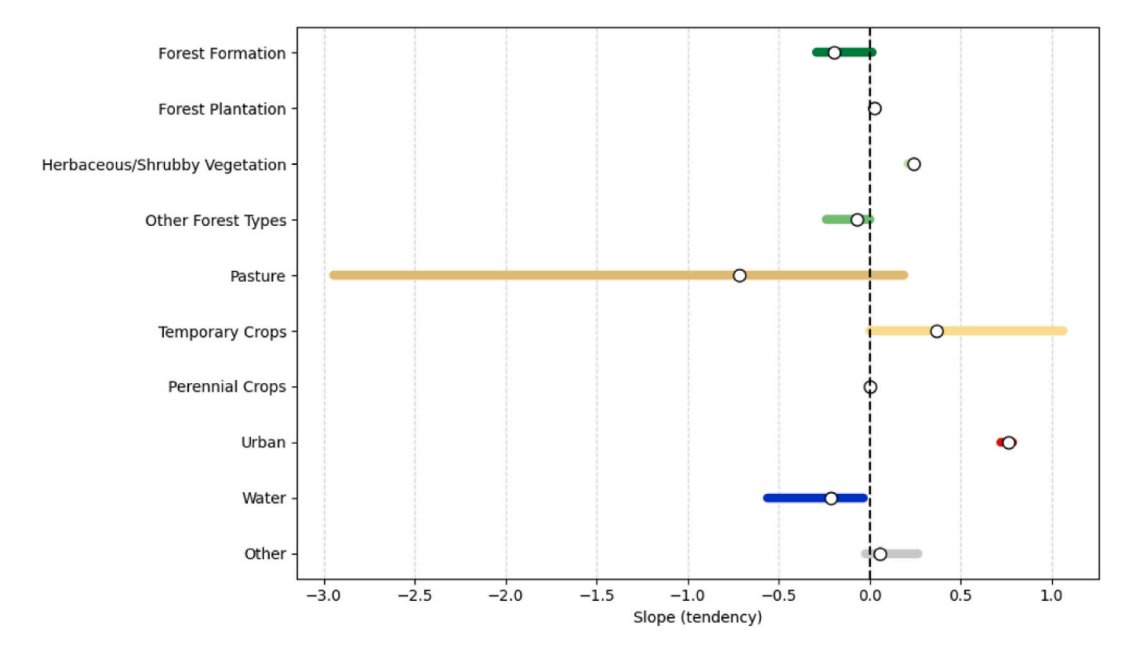


Fig. 7. Posterior distributions of slope estimates (tendency) for each land-use and land-cover class between 1985 and 2024. The horizontal bars represent the 95 % highest density intervals (HDI), while white dots indicate the posterior mean. The dashed vertical line represents the null effect (slope = 0).

exhibit relatively stable annual changes, corroborating the gradual but steady gains identified in the period averages.

Overall, the results indicate that pasture contraction and urban expansion are the dominant processes shaping land-use change in Hilltop APPs. Forest Formation has shown moderate permanence with small but consistent increases, while Forest Plantations emerge as a recent but rapidly expanding land-use category. The pronounced interannual variability, particularly in pastures and transitional classes, underscores that, beyond clear long-term trends, isolated episodes of abrupt area loss or gain significantly contribute to the dynamics of land-use change in these protected landscapes.

# 3.4.2. Bayesian analysis by MCMC with the NUTS algorithm in hilltop areas of Petrópolis

The Bayesian analysis of LULC dynamics in hilltop APPs between 1985 and 2024 revealed heterogeneous trajectories across classes, with some stability in natural vegetation but pronounced signals of land use intensification and urban expansion. Forest Formation exhibited a slight positive trend(slope = 0.08; 95 % HDI: 0.01-0.16), with a 96 % probability of increase (Fig. 7). The temporal trajectory confirmed modest but continuous recovery (Fig. 8a), suggesting gradual reforestation or regeneration in these areas despite the reduced obligations imposed by the revised Forest Code.

Forest Plantations, in turn, showed the most robust expansion signal (slope = 0.24; 95 % HDI: 0.11–0.36; P[increase] = 1.00), concentrated in recent years. This sharp increase reflects the introduction of silvicultural activities in APPs, highlighting the regulatory loopholes that allowed productive uses even in environmentally sensitive zones. Herbaceous/Shrubby Vegetation revealed a slight negative tendency (slope =  $-0.08;\,95$  % HDI: 0.15–0.00; P[decrease] = 0.97), with its proportion declining steadily over time (Fig. 8a). This reduction is consistent with the replacement of degraded or transitional vegetation either by pastures in earlier decades or by secondary forest regeneration in recent periods.

Pastures displayed the strongest and most persistent decline (slope = -0.66; 95 % HDI: 1.24–0.09; P[decrease] = 0.99; Fig. 7). Their proportion fell sharply (Fig. 8a), with probabilities of decrease equal to one

across most years (Fig. 8b). This pattern indicates systematic replacement of pastures by forest regrowth, plantations, or urban expansion, evidencing a major restructuring of land uses in hilltop APPs.

Temporary Crops showed high uncertainty, with slope estimates overlapping zero (slope = 0.05; 95 % HDI: 0.12–0.38), and posterior probabilities close to equilibrium (P[increase] = 0.52; Fig. 7). The temporal evolution (Fig. 8a) highlighted oscillations rather than consistent growth, reflecting short-term agricultural strategies and opportunistic use of restricted lands. Perennial Crops presented a weak tendency toward decline (slope = -0.09; 95 % HDI: 0.23–0.04; P [decrease] = 0.84), confirmed by their progressive reduction in the landscape (Fig. 8a). This trend suggests substitution by more profitable annual crops or urban land uses.

Urban areas presented the most unequivocal growth trend (slope = 0.19; 95 % HDI: 0.14–0.24; P[increase] = 1.00; Fig. 7). Their temporal trajectory shows continuous expansion (Fig. 8a), with probabilities of increase equal to one throughout the entire period (Fig. 8b). This consolidated trajectory underscores the anthropogenic pressure on hilltop APPs and reveals that the revised Forest Code has not curtailed urban occupation. Water areas and "Other" categories showed variable but generally negative tendencies, with limited influence on broader land-use dynamics.

Overall, the results demonstrate a dual dynamic: on one hand, Forest Formation and Forest Plantations expanded, suggesting regeneration and productive intensification; on the other, pastures declined markedly, while urban areas grew without interruption. These findings highlight that, despite the resilience of forest cover, hilltop APPs have been increasingly shaped by human occupation, with regulatory changes enabling both the persistence of natural recovery and the consolidation of urban expansion.

#### 3.5. Socioeconomic impacts on Petropolis

The extreme precipitation event in Petrópolis in February 2022 directly affected 1,078 people and caused more than USD 22 million of economic losses, being divided into USD 14 million were private losses (65.59 % of total), USD 1.8 million of public losses (8.28 %), and USD 5.7 million of material damage (26.13 %) (Table 4). The most affected sector was the commerce/services, accounting for 65.36 % of all losses, followed by dwellings, which represented 15.69 % of the total loss.

<sup>&</sup>lt;sup>2</sup> Quote as of September 11, 2025.

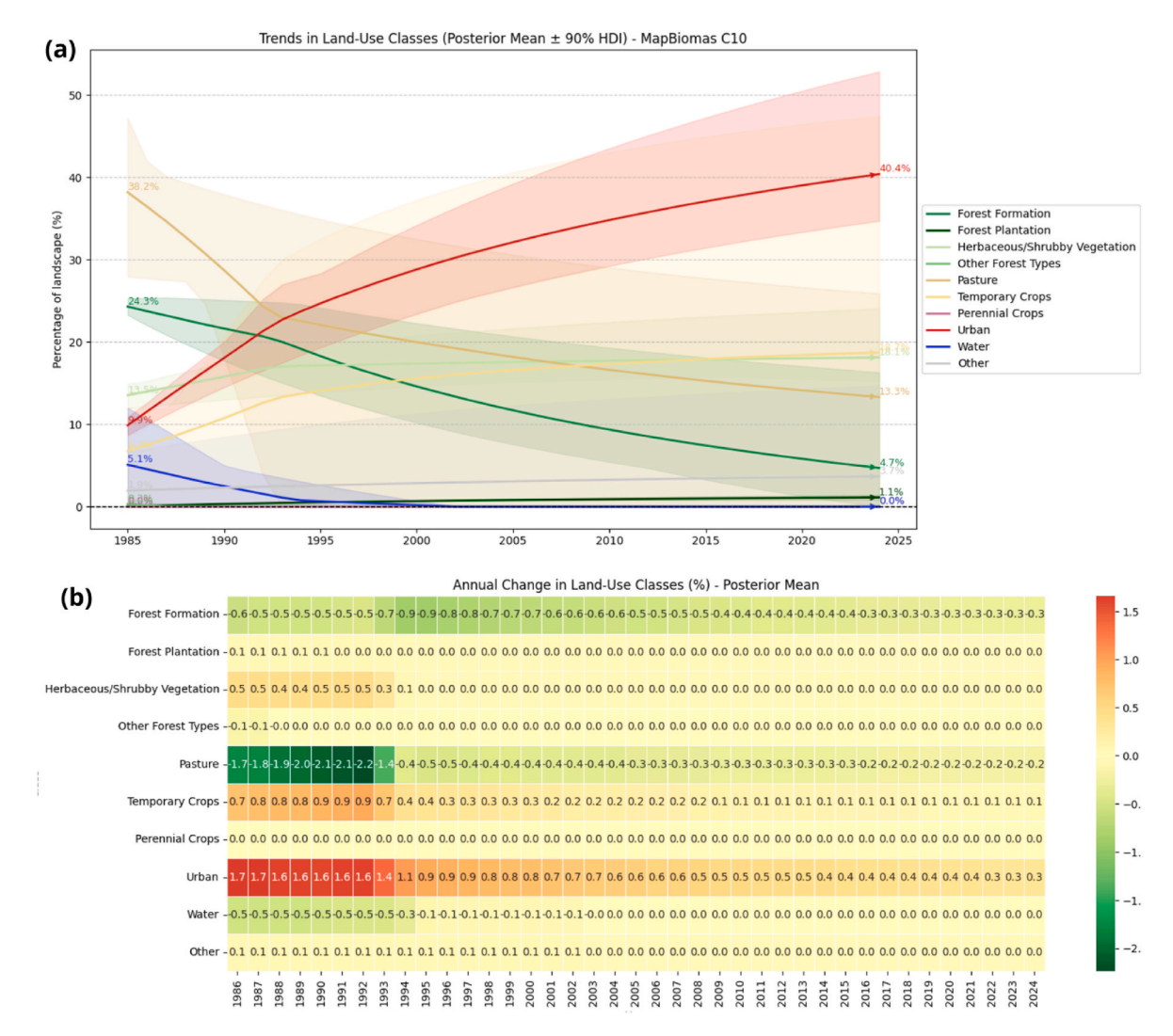


Fig. 8. Temporal dynamics of land-use and land-cover classes. (a) Evolution of the proportion of each class in the landscape, with shaded areas representing 95 % uncertainty intervals. (b) Posterior probabilities of increase for each class across the study period, ranging from 0 (probability of decrease) to 1 (probability of increase).

These values show the disruptions of services and losses of private and public properties, which can take weeks, months, or even years to be fully recovered or become permanent losses.

Concerning the human impacts, officially, 78 people were reported dead, 450 were sick or injured, and 450 lost their homes or had to be displaced (Table 4). However, these data were collected from the Municipal Civil Defense, which registers the impact at the moment of the disaster, underestimating the total human impact since it may require long-term assessment due to the local capacity to perform the necessary work. The National Civil Defense reported that at least 240 people died.

# 4. Discussion

The extreme precipitation event during the austral summer of 2021–2022 in Southeastern Brazil, particularly across Minas Gerais, Rio de Janeiro, and São Paulo states, was characterized by exceptional accumulated rainfall over multiple temporal scales. CPC data indicated maximum aggregated totals of approximately 225 mm for three days (Rx3day), 510 mm for thirty days (Rx30day), and 850 mm for sixty days (Rx60day). Moreover, bias adjustments were applied to correct systematic underestimation in the HadGEM3-A models (both ALL and NAT), especially over the 30- and 60-day scales. Data normalization against the 1981–2013 climatology (ratio of event value to historical

mean) enabled more consistent inter-scenario comparisons. Subsequently, the Generalized Extreme Value (GEV) distribution was fitted to the indices, demonstrating good goodness-of-fit and enabling reliable estimation of exceedance probabilities under both anthropogenic-forced (ALL) and natural-only (NAT) scenarios.

Attribution studies focused on extreme rainfall events in Brazil remain relatively limited, particularly in the Southeastern region, yet they consistently indicate increased probabilities of extreme precipitation across several areas of South America due to anthropogenic climate change (De Abreu, 2019; Rudorff et al., 2021; Dalagnol et al., 2022; Zachariah et al., 2022; das Junior, 2024; de Souza et al., 2024; Quevedo et al., 2023, 2025). For instance, Rudorff et al. (2021) estimated up to a 30 % increase in flood probability in the Parnaíba River basin attributable to global warming. Specifically in Southeastern Brazil, Dalagnol et al. (2022) demonstrated that the extreme event affecting Minas Gerais in 2020 became 70 % more likely due to anthropogenic influence. Also, De Souza et al. (2024), in investigating the extreme rainfall event that occurred in the Baixada Santista region (São Paulo), which was also associated with widespread landslides, showed through the analysis of two metrics - Rx60day (extreme 60-day accumulated rainfall), associated with antecedent soil moisture conditions, and Rx3day (extreme 3-day accumulated rainfall), related to landslide-triggering rainfall that the event became more likely due to anthropogenic climate change.

**Table 4**Socioeconomic impacts as a consequence of the extreme precipitation event. The economic losses show the most impacted sectors related to private economic losses, public economic losses, and material damage. The human losses (number of people) include the homeless and displaced, sick and injured, and deaths.

Economic impacts (	USD) <sup>a,b,c</sup>		Total <sup>d</sup>
Private Losses <sup>d</sup>	Commerce/services	\$ 14,425,575.00	\$14,473,660.25
	Agriculture	\$ 48,085.25	
Public Losses <sup>d</sup>	Urban cleaning	\$471,235.45	\$1,827,239.50
	Water supply	\$240,426.25	
	Sewage system	\$932,853.85	
	Health Care	\$182,723.95	
Material Damage <sup>d</sup>	Public Infrastructure	\$2,305,206.88	\$5,767,344.88
	Dwellings	\$3,462,138.00	
Human impacts <sup>a,b,c</sup>			Total <sup>e</sup>
Homeless and displa	nced <sup>e</sup>	450	1 078
Sick and injurede		550	
Deaths <sup>e</sup>		78	

<sup>&</sup>lt;sup>a</sup> Source: FIDE, 16/02/2022.

The Rx60day metric showed a 74 % increase in the probability of occurrence, while Rx3day became 46 % more likely under anthropogenic forcings. Additionally, Lyra et al. (2018) indicated that climate model projections show increases in the R95p and R99p indices across mountainous areas that encompass our study area, which may contribute to a higher frequency of mass movement events. Similar international findings corroborate the pivotal role of climate change in exacerbating disaster risks, with an increase in extreme precipitation across most of Europe, for example (Christidis and Stott, 2022; Hu et al., 2023).

These findings reinforce the conclusions of the latest IPCC Assessment Report (AR6), which states that the Southeastern South America (SES) region has experienced an estimated 19 % increase in extreme precipitation events since 1950 (low confidence) (IPCC, 2021). This upward trend is associated with a significant rise in the frequency of landslides and flash floods (Castellanos et al., 2022) — events that have led to a high number of fatalities in Brazil (high confidence) (Debortoli et al., 2017; Haque et al., 2019; Fonseca Aguiar and Cataldi, 2021), as exemplified by the 2022 disaster in Petrópolis, analyzed in this study. Altogether, this body of evidence supports the hypothesis that global warming has intensified both the magnitude of extreme rainfall and the persistence of antecedent soil moisture, a critical combination that amplifies the risk of landslides and flooding.

## 4.1. Variation in landslide damage of 2024

The dynamics of land use in landslide-prone areas of Petrópolis (Fig. 9) reveal an intensification of urban pressure over the last four decades. The Sankey diagram (Fig. S1a) shows that, between 1985 and 2022, a substantial flow of areas previously occupied by pastures and Forest Formation was converted into urban land. While Forest Formation and Other Forest Types maintained part of their extent, their relative contribution diminished as urban expansion accelerated, particularly after 2012. This shift coincides with the revision of the Brazilian Forest Code, which reduced restoration requirements in APPs and allowed the consolidation of pre-existing occupations on steep

slopes, thereby facilitating the permanence and growth of settlements in high-risk zones.

The bar chart (Fig. S1b) confirms that, in absolute terms, urban areas expanded markedly and became the dominant land-cover class by 2022. In contrast, pastures declined, and forest-related categories remained relatively constant in extent but lost proportional relevance. The proportional analysis (Fig. S1c) reinforces this interpretation: while urban land increased sharply, forests and natural vegetation decreased in relative share, reflecting a structural reconfiguration of land cover in landslide-prone environments.

These results highlight that urbanization is the primary driver of LUCC in Petrópolis, exacerbating risks associated with slope instability. The decline in the relative importance of forests and natural vegetation implies a reduction in protective ecosystem services, potentially intensifying erosion and slope failure. Agricultural uses, including temporary and perennial crops, remained marginal and did not significantly influence recent LULC dynamics.

These results indicate that urbanization is the main driver of LUCC in landslide-prone zones, amplifying risks associated with slope instability. The reduction in the relative contribution of forest and natural vegetation implies a loss of protective cover, which could exacerbate soil erosion and slope failure. Meanwhile, agricultural uses remain marginal and relatively stable, suggesting that they are not central to recent LULC dynamics in these high-risk environments. Overall, the findings emphasize the importance of integrating urban growth control and slope stabilization policies in Petrópolis. The persistence of forest classes suggests potential for ecosystem-based risk reduction, but the unchecked expansion of urban areas into steep and fragile terrains, particularly after the 2012 regulatory changes, poses significant challenges for disaster risk management.

Overall, the findings underscore the urgent need to integrate urban growth control with ecosystem-based approaches to slope stabilization. The persistence of forest classes points to a residual potential for ecological restoration and risk mitigation. However, the unchecked expansion of urban areas into steep and fragile terrains—particularly after the 2012 regulatory changes—represents a major challenge for disaster risk governance in Petrópolis.

# 4.2. Implications for disaster Prevention and adaptation policies

Historical LUCC have directly influenced disaster recurrence in Petrópolis. Three main classes were identified: natural formations, agricultural lands, and urban zones. Although there has been an aggregate increase in natural vegetation—likely linked to reforestation initiatives (Côrtes, 2017; Quevedo et al., 2023)—areas affected by landslides disproportionately encompass agricultural and urban uses. This aligns with evidence indicating that deforested areas for cultivation (Mugagga et al., 2012) or urban development (Vuillez et al., 2018; Liu et al., 2021) are more susceptible to landslides.

LULC transformations alter soil physical properties such as infiltration and cohesion, thereby impacting slope stability (Lehmann et al., 2019). Native vegetation enhances stability via root reinforcement (Masi et al., 2021; Parra et al., 2021), whereas replacement by crops increases vulnerability over time, especially post root decay (Soma et al., 2019).

Furthermore, lack of protection for hilltops—classified as APPs under the Brazilian Forest Code—compromises environmental integrity and exacerbates slope instability. Legal relaxations enacted in 2012 and 2014 (Magdalena et al., 2022) exempted municipal authorities from safeguarding these zones, contributing to altered runoff patterns and sediment dynamics.

The 2022 disaster resulted in 78 officially confirmed fatalities and economic losses exceeding USD 22 million, approximately 7.5 % of Petrópolis' municipal budget (Brasil, 2023). Unofficial estimates suggest even higher impacts (240 deaths, 1,178 displaced), but data inconsistencies fuel public distrust and hinder planning. Long-term

<sup>&</sup>lt;sup>b</sup> These data represent the preliminary damage survey up to 5:00 p.m. on 02/16/2022 (first 24 h). FIDE does not specify what damages and losses were due to the landslide. In the sheet, it is only described that the heavy rainfall caused landslides, floods, and other consequences.

<sup>&</sup>lt;sup>c</sup> Urban areas with affected populations: Quitandinha, Centro, Alto da Serra, Mosela, Independência, Estrada da Saudade, São Sebastião, Morin, Castelânea, Bairro Castrioto, Caxambu, Chácara Flora, Corrêa, Fazenda. Rural area: Caxambu, Santa Isabel.

 $<sup>^{\</sup>rm d}\,$  All values are expressed in USD (EUA currency) - Quote from February 13th, 2023.

e Number of people.

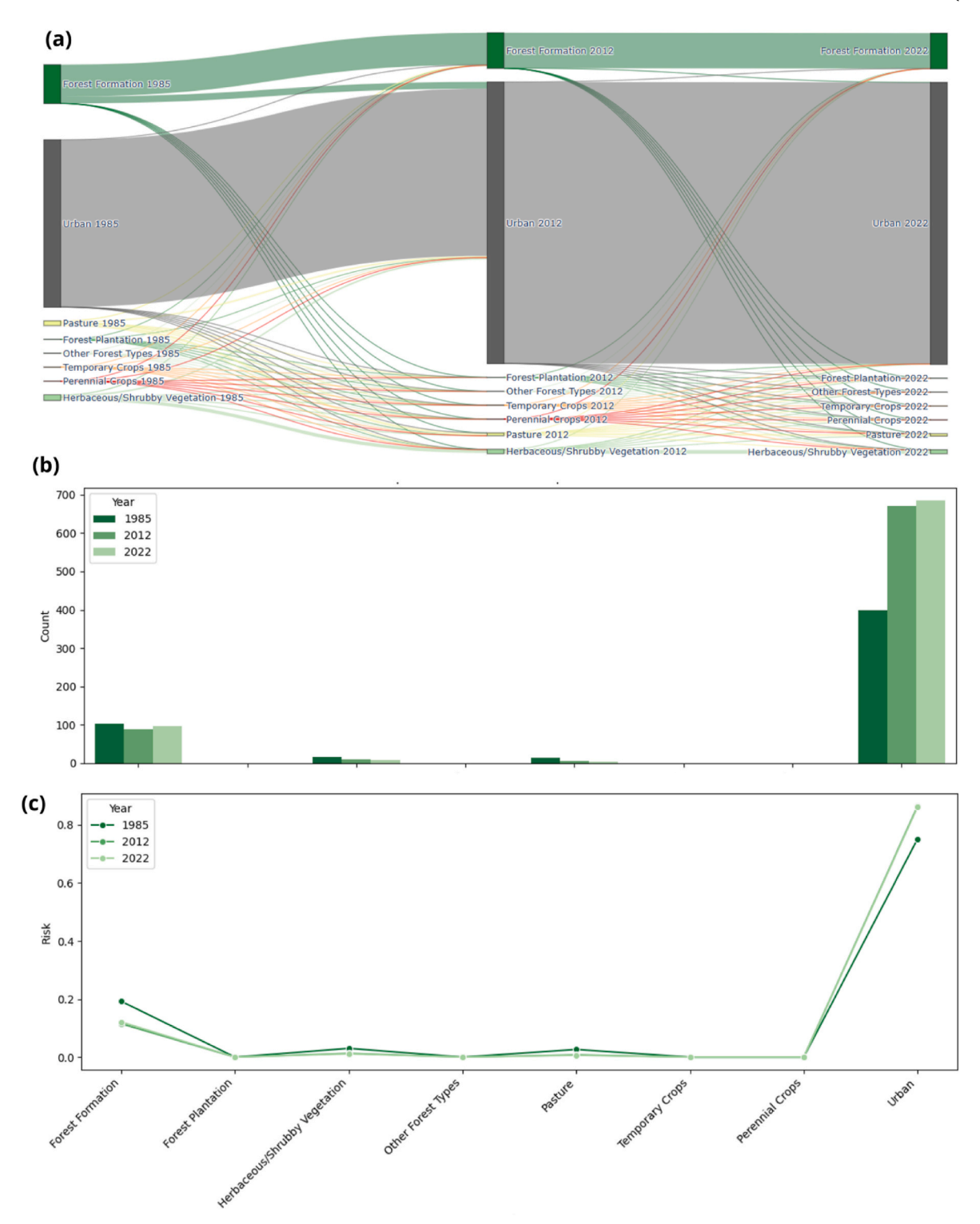


Fig. 9. Land use and land cover (LULC) dynamics in landslide-prone areas of Petrópolis. (a) Sankey diagram illustrating transitions among LULC classes between 1985, 2012, and 2022. (b) Distribution of total area (km²) occupied by each class in the three time points. (c) Relative share of each land cover class in landslide-prone zones, highlighting proportional changes across time.

repercussions—psychological trauma, food insecurity, and cultural heritage loss—are frequently unrecorded in platforms like S2ID, exposing institutional fragilities in national risk management.

# 4.3. Limitations of the HadGEM3-A model and FAR metric

While HadGEM3-A is widely employed in attribution studies for its

capacity to simulate anthropogenic (ALL) and natural-only (NAT) forcing scenarios, it has notable constraints. The atmospheric-only configuration features limited surface coupling, restricting representation of coupled oceanic and terrestrial feedback such as local evapotranspiration and soil moisture persistence, which are vital processes to the 2021–2022 events. Also, the horizontal resolution of the model (approximately 60 km) is coarse to effectively represent the rainfall that

triggered the specific landslide; however, it still can reproduce the regional to large-scale conditions for precipitation that led to the event.

Moreover, the FAR metric, while intuitive, has methodological limitations. Its estimates depend on the choice of thresholds, the statistical distribution fit (here, GEV), and data quality. Small uncertainties in distribution tails can substantially alter attribution values. FAR also does not differentiate between distinct physical drivers of risk increase—such as temperature rise versus changes in atmospheric circulation patterns—and thus lacks mechanistic diagnostic power. To strengthen inference, triangulation with complementary metrics, such as the Risk Ratio (RR), and high-resolution coupled model experiments incorporating key local and regional processes, is recommended.

#### 5. Conclusions

This study presents the first attribution analysis of the February 2022 extreme precipitation event that triggered multiple landslides in Petrópolis, Brazil. Trends in land use and land cover changes (LUCC) and socioeconomic impacts were also quantified. Anthropogenic climate change increased the likelihood of this event by at least 45 % (Rx3day) and 71 % (Rx60day), reducing the recurrence intervals from 2.36 to 1.63 years (short term) and 5.66 to 3.31 years (long term).

Although forest cover has increased, critical areas such as hilltops remain highly converted to agriculture (>40 %), increasing landslide susceptibility and necessitating targeted protection. The socioeconomic impact includes over USD 22 million in losses and more than 1,000 people affected. Petrópolis has a long history of disaster events, with major incidents driving improvements in civil defense. However, the 2022 event exposed ongoing gaps in preparedness intensified by climate change. This study highlights the need for further event attribution research and comprehensive impact assessments to inform effective climate adaptation and disaster risk reduction policies.

# CRediT authorship contribution statement

Maria Lucia Ferreira Barbosa: Conceptualization, Data curation, Formal analysis, Investigation, Methodology, Software, Validation, Visualization, Writing - original draft, Writing - review & editing. Rafaela Quintella Veiga: Conceptualization, Data curation, Formal analysis, Investigation, Methodology, Software, Validation, Visualization, Writing - original draft, Writing - review & editing. Renata Pacheco Quevedo: Conceptualization, Data curation, Formal analysis, Investigation, Methodology, Software, Validation, Visualization, Writing - original draft, Writing - review & editing. Débora Joana Dutra: Conceptualization, Data curation, Formal analysis, Investigation, Methodology, Software, Validation, Visualization, Writing - original draft, Writing - review & editing. Ana Carolina Moreira Pessôa: Conceptualization, Data curation, Formal analysis, Investigation, Methodology, Software, Validation, Visualization, Writing - original draft, Writing - review & editing. Thaís Pereira de Medeiros: Data curation, Formal analysis, Investigation, Methodology, Software, Validation, Visualization, Writing - original draft. Chantelle Burton: Conceptualization, Data curation, Formal analysis, Investigation, Methodology, Software, Validation, Visualization, Writing - original draft. Yuexiao Liu: Conceptualization, Data curation, Formal analysis, Investigation, Methodology, Software, Validation, Visualization, Writing - original draft. Nubia Beray Armond: Conceptualization, Data curation, Formal analysis, Investigation, Methodology, Software, Validation, Visualization, Writing - original draft. Rafael C. de Abreu: Conceptualization, Data curation, Formal analysis, Investigation, Methodology, Project administration, Software, Supervision, Validation, Visualization, Writing – original draft, Writing – review & editing. Sihan Li: Conceptualization, Data curation, Formal analysis, Investigation, Methodology, Project administration, Software, Supervision, Validation, Visualization, Writing - original draft, Writing - review & editing. Fraser C. Lott: Conceptualization, Data curation, Formal analysis,

Investigation, Methodology, Resources, Supervision, Writing – original draft, Writing – review & editing. Cassiano Antonio Bortolozo: Data curation. Sarah Sparrow: Conceptualization, Data curation, Formal analysis, Funding acquisition, Investigation, Methodology, Project administration, Supervision, Writing – original draft, Writing – review & editing. Liana Oighenstein Anderson: Conceptualization, Data curation, Formal analysis, Funding acquisition, Investigation, Methodology, Project administration, Resources, Supervision, Writing – original draft, Writing – review & editing.

#### Declaration of competing interest

The authors declare that they have no known competing financial interests or personal relationships that could have appeared to influence the work reported in this paper.

#### Acknowledgements

This study was derived from the Attribution and Synopsis of Landslide Impacts from Precipitation (ASLIP) 2022 workshop, supported by the Newton Fund through the Met Office Climate Science for Services Partnership Brazil (CSSP Brazil) and organized by Drs. Sarah Sparrow, Fraser Lott, Liana Anderson, Sihan Li, and Rafael de Abreu. We thank the JASMIN team and the Centre for Environmental Data Analysis (CEDA) for providing the computational infrastructure used for data processing. We would like to thank Imagery © 2022 Planet Labs Inc., made available by the NICFI (Norway's International Climate and Forest Initiative) and National Institute for Space Research- Brazil (INPE) for providing images of the Geo-Eye-1 satellite data. This study was financed in part by the Coordenação de Aperfeiçoamento de Pessoal de Nível Superior -Brasil (CAPES) - Finance Code 001. CB was supported by the Newton Fund through the Met Office Climate Science for Services Partnership Brazil (CSSP Brazil). For Open Access, the author has applied a CC BY public copyright license to any Author Accepted Manuscript (AAM) version arising from this submission.

# Appendix A. Supplementary data

Supplementary data to this article can be found online at https://doi.org/10.1016/j.wace.2025.100811.

#### Data availability

The data that support the findings of this study are all publicly available from their sources. The HadGEM3-A data is available upon request to the MetOffice (fraser.lott@metoffice.gov.uk). Processed data and code produced in this study are available from the corresponding author upon reasonable request. The land use code and dataset can be access by Zenodo (https://zenodo.org/records/17154445).

#### References

Alawamy, E.A., Liu, Y., Zhao, Y.Q., 2022. Bayesian analysis for single-server Markovian queues based on the No-U-Turn sampler. Commun. Stat. Simulat. Comput. 51 (2), 658–670. https://doi.org/10.1080/03610918.2022.2025841.

Alcântara, E., Marengo, J.A., Mantovani, J., Londe, L., San, R.L.Y., Park, E., Lin, Y.N., Mendes, T., Cunha, A.P., Pampuch, L., Seluchi, M., 2023. Deadly disasters in Southeastern South America: flash floods and landslides of February 2022 in Petrópolis, Rio de Janeiro. Nat. Hazards Earth Syst. Sci. Disc. 1–27. https://doi.org/10.5194/nhess-23-1157-2023.

Allen, M., 2003. Liability for climate change. Nature 421 (6926), 891–892. https://doi. org/10.1038/421891a.

Ambrozio, J.C.G., 2008. O Presente E O Passado No Processo Urbano Da Cidade De Petrópolis. Thesis. (Doctorate in Human Geography - Faculty of Philosophy, Letters and Human Sciences, University of São Paulo, São Paulo. https://doi.org/10.11606/T.8.2008.tde-06012009-163050.

Antunes, F.S., Fernandes, M.C., 2020. Análise geográfica e cartografia histórica: subsídios para entender a organização espacial da área gênese de Petrópolis (RJ). Geousp 24 (1), 117–135. https://doi.org/10.11606/issn.2179-0892.geousp.2020.148942.

- BRASIL. Instrução Normativa N° 36 de 4 de dezembro de, 2020. Estabelece procedimentos e critérios para o reconhecimento federal e para declaração de situação de emergência ou estado de calamidade pública pelos municípios, estados e pelo Distrito Federal, 25 ed. Ministério do Desenvolvimento Reg., p 21 section 1.
- BRASIL, 2023. Controladoria-Geral Da União. Portal Da Transparência: Órgãos 2023. Brasília. Disponível em: https://portaldatransparencia.gov.br/orgaos?ano=2023.
- Câmara Municipal de Petrópolis, 2022. Diário Oficial da Câmara. https://www.petropolis.rj.leg.br/leis/diario-oficial-da-camara/2022/junho/do-21-06-2022.pdf.
- Cardozo, C.P., Monteiro, A.M.V., 2019. Assessing social vulnerability to natural hazards in Nova Friburgo, Río de Janeiro mountain region, Brazil. Revista de Estudios Latinoamericanos sobre Reducción del Riesgo de Desastres (REDER) 3 (2), 71–83. Available at: https://www.aacademica.org/paola.cardozo/2.pdf.
- Carlson, C.J., Mitchell, D., Carleton, T., Chersich, M., Gibb, R., Lavelle, T., et al., 2024. Designing and describing climate change impact attribution studies: a guide to common approaches. https://doi.org/10.31223/X5CD7M.
- Castellanos, et al., 2022. Central and South America. In: Pörtner, H.-O., Roberts, D.C., Tignor, M., Poloczanska, E.S., Mintenbeck, K., Alegría, A., Craig, M., Langsdorf, S., Löschke, S., Möller, V., Okem, A., Rama, B. (Eds.), Climate Change 2022 Impacts, Adaptation and Vulnerability: Working Group II Contribution to the Sixth Assessment Report of the Intergovernmental Panel on Climate Change, first ed. Cambridge University Press, Cambridge, UK and New York, NY, USA, pp. 1689–1816. https://doi.org/10.1017/9781009325844.014. Cambridge University Press.
- Christidis, N., Stott, P.A., 2022. The extremely wet May of 2021 in the United Kingdom.

  Bull. Amer. Meteor. Soc. 103, E2912–E2916. https://doi.org/10.1175/BAMS-D-22-0108.1
- Chen, M., Shi, W., Xie, P., Silva, V.B.S., Kousky, V.E., Wayne Higgins, R., Janowiak, J.E., 2008. Assessing objective techniques for gauge-based analyses of global daily precipitation. J. Geophys. Res. Atmos. 113 (D4). https://agupubs.onlinelibrary.wilev.com/doi/abs/1.
- Cohen, D., Schwarz, M., 2017. Tree-root control of shallow landslides. Earth Surf. Dyn. 5 (3), 451–477. https://doi.org/10.5194/esurf-5-451-2017.
- Ciavarella, Andrew, et al., 2018. Upgrade of the HadGEM3-A based attribution system to high resolution and a new validation framework for probabilistic event attribution. Weather Clim. Extrem. 20, 9–32.
- Côrtes, R.T., 2017. Produção Florestal e Agricultura Familiar: o Caso da Região Serrana Fluminense [Universidade Federal Rural do Rio de Janeiro]. https://tede.ufrrj.br/ jspui/bitstream/jspui/2445/2/2017-RaíssaTamassiaCôrtes.pdf.
- Costa, M.A.M., Fogaça, I.D.F., Moraes, C.C.D.A., 2022. Reflexões sobre o turismo em Petrópolis-RJ: impactos da Covid-19 e das chuvas no verão de 2022. GEOUSP 26, e200963
- Dalagnol, R., et al., 2022. Extreme rainfall and its impacts in the Brazilian Minas Gerais state in January 2020: can we blame climate change? Clim. Resil. Sustain. 1 (1), e15. https://doi.org/10.1002/cli2.15.
- Davies, T., Cullen, M.J.P., Malcolm, A.J., Mawson, M.H., Staniforth, A., White, A.A., Wood, N., 2005. A new dynamical core for the met office's global and regional modelling of the atmosphere. Q. J. R. Meteorol. Soc. 131 (608), 1759–1782. https://doi.org/10.1256/qj.04.101.
- De Abreu, R.C., et al., 2019. Contribution of anthropogenic climate change to April-May 2017 heavy precipitation over the Uruguay River Basin. Bull. Am. Meteorol. Soc. 100 (1), S37–S41.
- De Assis, D.M.C., Saito, S.M., dos Santos Alvalá, R.C., Stenner, C., Pinho, G., Nobre, C.A., de Souza Fonseca, M.R., Santos, C., Amadeu, P., Silva, D., Lima, C.O., 2018. Estimation of exposed population to landslides and floods risk areas in Brazil, on an intra-urban scale. Int. J. Disaster Risk Reduct. 31, 449–459. https://doi.org/10.1016/j.ijdrr.2018.06.002.
- De Souza, D.C., Crespo, N.M., da Silva, D.V., Harada, L.M., de Godoy, R.M.P., Domingues, L.M., et al., 2024. Extreme rainfall and landslides as a response to human-induced climate change: a case study at Baixada Santista, Brazil, 2020. Nat. Hazards 120 (12), 10835–10860.
- Debortoli, N.S., Camarinha, P.I.M., Marengo, J.A., Rodrigues, R.R., 2017. An index of Brazil's vulnerability to expected increases in natural flash flooding and landslide disasters in the context of climate change. Nat. Hazards 86, 557–582. https://doi. org/10.1007/s11069-016-2705-2.
- Dias, H.C., Hölbling, D., Grohmann, C.H., 2021. Landslide susceptibility mapping in Brazil: a review. Geosciences 11 (10), 425. https://doi.org/10.3390/ geosciences11100425.
- Dourado, F., Arraes, T.C., e Silva, M.F., 2012. The" Megadesastre" in the Mountain Region of Rio de Janeiro State: causes, mechanisms of mass movements and spatial allocation of investments for reconstruction post disaster. Anu. do Inst. Geociencias 35 (2), 43–54. https://doi.org/10.11137/2012\_2\_43\_54.
- Farr, T.G., Rosen, P.A., Caro, E., Crippen, R., Duren, R., Hensley, S., Kobrick, M., Paller, M., Rodriguez, E., Roth, L., Seal, D., Shaffer, S., Shimada, J., Umland, J., Werner, M., Oskin, M., Burbank, D. e, Alsdorf, D.E., 2007. The shuttle radar topography mission. Rev. Geophys. 45 (2). https://doi.org/10.1029/2005RG000183. RG2004, at.
- Frame, D.J., Rosier, S.M., Noy, I., Harrington, L.J., Carey-Smith, T., Sparrow, S.N., et al., 2020. Climate change attribution and the economic costs of extreme weather events: a study on damages from extreme rainfall and drought. Clim. Change 162 (2), 781–797. https://doi.org/10.1007/s10584-020-02729-y.
- Fonseca Aguiar, L., Cataldi, M., 2021. Social and environmental vulnerability in Southeast Brazil associated with the south Atlantic convergence Zone. Nat. Hazards 109 (3), 2423–2437. https://doi.org/10.1007/s11069-021-04926-z.
- Gariano, S.L., Guzzetti, F., 2016. Landslides in a changing climate. Earth Sci. Rev. 162, 227–252. https://doi.org/10.1016/j.earscirev.2016.08.011.

- Guerra, A.J.T., Gonçalves, L.F.H., Lopes, P.B.M., 2007. Evolução histórico-geográfica da ocupação desordenada e movimentos de massa no município de Petrópolis, nas últimas décadas. Revista Brasileira de Geomorfologia 8 (1).
- Haque, Ubydul, da Silva, Paula F., Devoli, Graziella, Pilz, Jürgen, Zhao, Bingxin, Khaloua, Asmaa, Wilopo, Wahyu, et al., 2019. The human cost of global warming: deadly landslides and their triggers (1995–2014). Sci. Total Environ. 682 (September), 673–684. https://doi.org/10.1016/j.scitotenv.2019.03.415.
- Hegerl, G.C., Hoegh-Guldberg, O., Casassa, G., Hoerling, M., Kovats, S., Parmesan, C., Pierce, D., Stott, P., 2010. Good practice guidance paper on detection and attribution related to anthropogenic climate change. In: Stocker, T.F., Field, C., Dahe, Q., Barros, V., Plattner, G.-K., Tignor, M., Pauline Midgley, P., Ebi, K. (Eds.), Meeting Report of the Intergovernmental Panel on Climate Change Expert Meeting on Detection and Attribution of Anthropogenic Climate Change. IB>Ipccrking Group I Technical Support Unit. University of Bern, Bern, p. 8.
- Hirabayashi, Y., Alifu, H., Yamazaki, D., et al., 2021. Anthropogenic climate change has changed the frequency of past floods during 2010-2013. Prog. Earth Planet. Sci. 8, 36. https://doi.org/10.1186/s40645-021-00431-w.
- Hu, T., et al., 2023. Anthropogenic influence on the 2021 wettest September in northern China. Bull. Am. Meteorol. Soc. 104 (1), E243–E248.
- IBGE Instituto Brasileiro de Geografia e Estatística, 2025. Panorama do município de Petrópolis (RJ). https://cidades.ibge.gov.br/brasil/rj/petropolis/panorama. (Accessed 15 May 2025).
- IPCC, 2021. Sumário para Formuladores de Políticas. In: Masson-Delmotte, V., Zhai, P., Pirani, A., Connors, S.L., Péan, C., Berger, S., Caud, N., Chen, Y., Goldfarb, L., Gomis, M.I., Huang, M., Leitzell, K., Lonnoy, E., Matthews, J.B.R., Maycock, T.K., Waterfield, T., Yelekçi, O., Zhou, R. Yu e B. (Eds.), Em Mudança do Clima 2021: A Base da Ciência Física. Contribuição do Grupo de Trabalho I ao Sexto Relatório de Avaliação do Painel Intergovernamental Sobre Mudanças Climáticas. Cambridge University Press, Cambridge. No prelo.
- das Junior, F.C.V., et al., 2024. An attribution study of very intense rainfall events in eastern Northeast Brazil. Weather Clim. Extrem., 100699
- Karandikar, R.L., 2006. On the Markov Chain Monte Carlo (MCMC) method. Sadhana 31 (2), 81–104. https://doi.org/10.1007/BF02719775.
- Kundzewicz, Z.W., Pińskwar, I., 2022. Are pluvial and fluvial floods on the rise? Water 14 (17), 2612. https://doi.org/10.3390/w14172612.
- Leach, N.J., Weisheimer, A., Allen, M.R., Palmer, T., 2021. Forecast-based attribution of a winter heatwave within the limit of predictability. Proc. Natl. Acad. Sci. 118 (49), e2112087118.
- Lehmann, P., von Ruette, J., Or, D., 2019. Deforestation effects on rainfall-induced shallow landslides: remote sensing and physically-based modelling. Water Resour.

  Res. 55 (11) 9962–9976. https://doi.org/10.1029/2019WR025233
- Res. 55 (11), 9962–9976. https://doi.org/10.1029/2019WR025233.

  Lima, K.C., Satyamurty, P., Fernández, J.P.R., 2010. Large-scale atmospheric conditions associated with heavy rainfall episodes in southeast Brazil. Theor. Appl. Climatol. 101 (1–2), 121–135. https://doi.org/10.1007/s00704-009-0207-9.
- Lima, A.O., Lyra, G.B., Abreu, M.C., Oliveira-Júnior, J.F., Zeri, M., Cunha-Zeri, G., 2021. Extreme rainfall events over Rio de Janeiro State, Brazil: characterization using probability distribution functions and clustering analysis. Atmos. Res. 247, 105221.
- Liu, J., Wu, Z., Zhang, H., 2021. Analysis of changes in landslide susceptibility according to land use over 38 years in Lixian county, China. Sustainability 13 (19), 1–23. https://doi.org/10.3390/su131910858.
- Lyra, Andre, Tavares, Priscila, Chan Chou, Sin, Sueiro, Gustavo, Dereczynski, Claudine, Sondermann, Marcely, Silva, Adan, Marengo, José, Giarolla, Angélica, 2018. Climate change projections over three metropolitan regions in southeast Brazil using the non-hydrostatic eta regional climate model at 5-Km resolution. Theor. Appl. Climatol. 132 (1), 663–682. https://doi.org/10.1007/s00704-017-2067-z.
- Magdalena, U.R., Francisco, C.N., Lopes, L.G., Rodriguez, D.A., 2022. Conservation policy changes in protected areas on hilltops in Brazil: effects on hydrological response in a small watershed. Water Resour. Manag. 36 (4), 1251–1270. https://doi.org/10.1007/s11269-022-03079-3.
- Masi, E.B., Segoni, S., Tofani, V., 2021. Root reinforcement in slope stability models: a review. Geosciences 11 (5), 212. https://doi.org/10.3390/geosciences11050212.
- Mugagga, F., Kakembo, V., Buyinza, M., 2012. Land use changes on the slopes of Mount Elgon and the implications for the occurrence of landslides. Catena 90, 39–46. https://doi.org/10.1016/j.catena.2011.11.004.
- Nemeth, C., Fearnhead, P., 2021. Stochastic gradient markov chain Monte Carlo. J. Am. Stat. Assoc. 116 (533), 433–450. https://doi.org/10.1080/ 01621459.2020.1847120.
- Netto, A.L.C., Fernandes, M., Nunes, F., Bertassoni, G., Bolsas, L., Facadio, A.C., e Silva, I. M., De Paula, A., Duek, T., Thaumaturgo, G., Moreno, L., 2022. The most recent disaster related to extreme rainfall induced landslides and floods: petropolis, Rio de Janeiro state, SE-Brazil (No. ICG2022-628). Copern. Meet. https://doi.org/10.5194/icg2002-628.
- Neto, G.G.R., Anderson, L.O., Barretos, N.J.C., Abreu, R., Alves, L., Dong, B., Lott, F.C., Tett, S.F.B., 2021. Attributing the 2015/2016 Amazon basin drought to anthropogenic influence. Clim. Resil. Sustain. 1 (1), e25. https://doi.org/10.1002/ clip. 25
- Nishio, M., Arakawa, A., 2019. Performance of Hamiltonian Monte Carlo and No-U-Turn sampler for estimating genetic parameters and breeding values. Genet. Sel. Evol. 51 (1), 73. https://doi.org/10.1186/s12711-019-0515-1.
- Otto, F.E.L., Coelho, C.A.S., King, A., Perez, E.C.D., Wada, Y., Oldenborgh, G.J.V., Haarsma, R., Haustein, K., Uhe, P., Aalst, M.V., Aravequia, J.A., Almeida, W., Cullen, H., 2015. Factors other than climate change, main drivers of 2014/15 water shortage in southeast Brazil. Am. Meteorol. Soc. S35–S40.
- Otto, F.E.L., van Oldenborgh, G.J., Eden, J., Stott, P.A., Karoly, D.J., Allen, M.R., 2016. The attribution question. Nat. Clim. Change 6 (9), 813–816. https://doi.org/

- Otto, F.E.L., 2017. Attribution of weather and climate events. Annu. Rev. Environ. Resour. 42 (1), 627–646. https://doi.org/10.1146/annurev-environ-102016-06047
- Parra, E., Mohr, C.H., Korup, O., 2021. Predicting patagonian landslides: roles of forest cover and wind speed. Geophys. Res. Lett. 48 (23), 1–10. https://doi.org/10.1029/ 2021GL095224.
- Pereira, D.R., Almeida, A.Q., Martinez, M.A., Rosa, D.R.Q., 2014. Impacts of deforestation on water balance components of a watershed on the Brazilian east Coast. Rev. Bras. Ciência do Solo 38 (4), 1353–1361. https://doi.org/10.1590/ S0100-06832014000400030.
- Perkins-Kirkpatrick, S.E., Stone, D.A., Mitchell, D.M., Rosier, S., King, A.D., Lo, Y.T.E., Pastor-Paz, J., Frame, D., Wehner, M., 2022. On the attribution of the impacts of extreme weather events to anthropogenic climate change. Environ. Res. Lett. 17 (2), 024009.
- Prefeitura, P., 2019. Turismo de negócios movimenta mais de R\$ 500 milhões em Petrópolis. Petrópolis 29, abr. Available at: https://www.petropolis.rj.gov.br/pmp/index.php/imprensa/noticias/item/12868-turismo-de-neg%C3%B3cios-moviment a-mais-de-r\$-500-milh%C3%B5es-em-petr%C3%B3polis.html. (Accessed 15 May 2025).
- Quevedo, R.P., Anderson, L.O., Horta, I.T.L.G., Velastegui-Montoya, A.D., Veiga, R.Q., Cardozo, C.P., Sparrow, S.N., 2023. The relationship between landslide occurrence and land use and land cover. In: CADERNO DE RESUMOS DO XX SIMPÓSIO BRASILEIRO DE SENSORIAMENTO REMOTO, 2023, Florianópolis. Anais Eletrônicos. São José dos Campos, INPE. Disponível em: https://proceedings.science/sbsr-2023/trabalhos/the-relationship-between-landslide-occurrence-and-land-use-and-land-cover?lang=en. (Accessed 14 March 2023).
- Quevedo, R.P., Ovando, A., Calado, B.N., Cunha-Zeri, G., da Silva, L.A., de Luna, Q.H.R., dos Santos, J.C., Abreu, R.C., Huang, W.T.K., Noronha, P., Leão, H., 2025.
  Attributing the 2021 Juruá river floods to climate change: evidence, impacts, and adaptation in the Brazilian Amazon. Int. J. Disaster Risk Reduct. 125, 105530. <a href="https://doi.org/10.1016/j.ijdrr.2025.105530">https://doi.org/10.1016/j.ijdrr.2025.105530</a>.
- Rosi, A., Canavesi, V., Segoni, S., Dias Nery, T., Catani, F., Casagli, N., 2019. Landslides in the mountain region of Rio de Janeiro: a proposal for the semi-automated definition of multiple rainfall thresholds. Geosciences 9 (5), 203. https://doi.org/ 10.3390/geosciences9050203.
- Rudorff, C., Sparrow, S., Guedes, M.R.G., Tett, S.F.B., Brêda, J.P.L.F., Cunningham, C., Ribeiro, F.N.D., Palharini, R.S.A., Lott, F.C., 2021. Event attribution of Parnaíba river floods in northeastern Brazil. Clim. Resil. Sustain. 1, e16. https://doi.org/10.1002/ cli2\_16
- S2ID, 2024. Sistema Integrado de Informações sobre Desastres. Available in: https://s2id.mi.gov.br/. (Accessed 19 December 2023).
- Seltzer, M.H., Wong, W.H., Bryk, A.S., 1996. Bayesian analysis in applications of hierarchical models: issues and methods. J. Educ. Behav. Stat. 21 (2), 131–167. https://doi.org/10.3102/10769986021002131.
- Schmid, C.H., Brown, E.N., 2000. Bayesian hierarchical models. Methods Enzymol. 321, 305–330. https://doi.org/10.1016/S0076-6879(00)21200-7.
- Soares, J., 2009. Petrópolis: ontem e hoje. Texto, Rio de Janeiro.

- Solman, S.A., Blázquez, J., 2019. Multiscale precipitation variability over South America: analysis of the added value of CORDEX RCM simulations. Clim. Dyn. 53, 1547–1565. https://doi.org/10.1007/s00382-019-04689-1.
- Soma, A.S., Kubota, T., Aditian, A., 2019. Comparative study of land use change and landslide susceptibility using frequency ratio, certainty factor, and logistic regression in upper area of Ujung-Loe watersheds South Sulawesi Indonesia. Int. J. Eros. Contr. Eng. 11 (4), 103–115. https://doi.org/10.13101/ijece.11.103.
- Souza Jr, C.M., Shimbo, J.Z., Rosa, M.R., Parente, L.L., Alencar, A.A., Rudorff, B.F., Hasenack, H., Matsumoto, M.G., Ferreira, L., Souza-Filho, P.W., de Oliveira, S.W., 2020. Reconstructing three decades of land use and land cover changes in brazilian biomes with landsat archive and earth engine. Remote Sens. 12 (17), 2735.
- Stott, P., Stone, D., Allen, M., 2004. Human contribution to the European heatwave of 2003. Nature 432, 610–614. https://doi.org/10.1038/nature03089.
- Stott, P.A., Christidis, N., Otto, F.E., Sun, Y., Vanderlinden, J.P., van Oldenborgh, G.J., Vautard, R., von Storch, H., Walton, P., Yiou, P., Zwiers, F.W., 2016. Attribution of extreme weather and climate-related events. Wiley Interdiscipl. Rev.: Clim. Change 7 (1), 23–41.
- Tavares, C.D.M.G., Ferreira, C.D.C.M., 2020. A Relação Entre a Orografia e os Eventos Extremos de Precipitação Para o Município De Petrópolis-RJ, vol. 26. Revista Brasileira de Climatologia.
- Vautard, R., Christidis, N., Ciavarella, A., et al., 2019. Evaluation of the HadGEM3-A simulations in view of detection and attribution of human influence on extreme events in Europe. Clim. Dyn. 52, 1187–1210. https://doi.org/10.1007/s00382-018-4183-6.
- Vieira, B.C., Gramani, M.F., 2015. Serra do Mar: the most "tormented" relief in Brazil. Landscapes and Landforms of Brazil, pp. 285–297. https://doi.org/10.1007/978-94-017-8023-0\_26.
- Vuillez, C., Tonini, M., Sudmeier-Rieux, K., Devkota, S., Derron, M.H., Jaboyedoff, M., 2018. Land use changes, landslides and roads in the Phewa Watershed, Western Nepal from 1979 to 2016. Appl. Geogr. 94 (March 2017), 30–40. https://doi.org/ 10.1016/j.apgeog.2018.03.003.
- Wang, Z., Jiang, Y., Wan, H., Yan, J., Zhang, X., 2017. Detection and attribution of changes in extreme temperatures at regional scale. J. Clim. 30 (17), 7035–7047. https://doi.org/10.1175/JCIJ-D-15-0835.1.
- Wang, J., Tett, S.F., Yan, Z., Feng, J., 2018. Have human activities changed the frequencies of absolute extreme temperatures in eastern China? Environ. Res. Lett. 13 (1), 014012. https://doi.org/10.1088/1748-9326/aa9404.
- Wang, Y., Wang, C., 2023. Classification of extreme heatwave events in the Northern hemisphere through a new method. Clim. Dyn. 1–23. https://doi.org/10.1007/ s00382-022-06649-8.
- Zachariah, M., das Chagas Vasconcelos Junior, F., Luiz do Vale Silva, T., Pereira dos Santos, E., Augusto dos Santos Coelho, C., Muniz Alves, L., Sávio Passos Rodrigues Martins, E., Köberle, A.C., Singh, R., Vahlberg, M., Marchezini, V., 2022. Climate change increased heavy rainfall, hitting vulnerable communities in eastern northeast Brazil. World Weather Attribut. Scient. Rep.
- Zobitz, J.M., Desai, A.R., Moore, D.J.P., Chadwick, M.A., 2011. A primer for data assimilation with ecological models using Markov Chain Monte Carlo (MCMC). Oecologia 167 (3), 599–611. https://doi.org/10.1007/s00442-011-2107-9.